Spring 5-2005

Novel Design of a Gradual Portosystemic Shunt Occluder

Elizabeth Ann Cushman
University of Tennessee - Knoxville

Mitchell Ryan Ladd
University of Tennessee- Knoxville

Geoffrey Ian Watson
University of Tennessee- Knoxville

Devin Lance Weinberg
University of Tennessee- Knoxville

Novel design of a gradual portosystemic shunt occluder

Devin Weinberg

Beth Cushman

Mitchell Ladd

Geoff Watson

Table of Contents

Background

A portosystemic shunt is a blood vessel that allows blood to bypass the liver, move directly into the inferior vena cava and then into the heart, thus eliminating the functionality of the liver. The liver is a vital organ as it functions in digestion, excretion, nutrient storage, nutrient conversion, detoxification, and synthesis capabilities. More specifically, its constitutive cells act in removal and storage of sugar from the blood as well as fat, vitamin, copper and iron storage. In addition, it removes elements such as ammonia and converts to a safer chemical form of nitrogen in urea, which is excreted from the body via the kidneys. The liver also prevents these toxins from reaching the heart and causing sepsis, which is potentially fatal. Furthermore, the liver creates necessary homeostatic blood proteins such as albumin, fibrinogen, globulins, and clotting factors.

In a normal functioning body system, the hepatic artery carries oxygen-rich blood to the liver to supply it with the necessary oxygen to perform its organ functions. The hepatic portal vein carries oxygen-poor blood that contains added materials from the digestive tract to the liver. The liver removes these materials from the oxygen-poor blood. Then the blood exits the liver through the hepatic veins and continues through the circulatory system.

In mammalian dogs, the ductus venosus is a large portosystemic shunt that circumvents the liver while in fetal development. Portosystemic shunts are classified based on three categories: method of development, structural integrity, and type of bypass. The development of portosystemic shunts is classified as either congenital or acquired. Congenital shunts are those that arise during fetal development and that fail to

degrade naturally. Acquired shunts occur out of a response to liver disease. For example, cirrhosis of the liver decreases its functionality and cause angiogenesis to assist in diverting blood away from a nonfunctional liver and to protect a damaged liver from further deterioration. Congenital shunts occur at a greater frequency and have been noted to be genetically linked in breeds including Maltese, Irish wolfhound, and presumably Yorkshire terriers. The two main structural classifications are extrahepatic and intrahepatic shunts. These classifications are based upon where the branching off the shunt occurs relative to the portal vein. If the base of the shunt begins at the main portal vein and then flows directly to the inferior vena cava, the shunt is classified as an extrahepatic portosystemic shunt (Figure 1(b) and Figure 2). Typically, these shunts vary in size as great as 1 cm in diameter. If the base begins within the branching of the portal vein, and then flows to the inferior vena cava, then it is classified as an intrahepatic portosystemic shunt. See Figure 1(c) for illustrations. The treatment of intrahepatic portosystemic shunts is not dealt with in the same way due to their smaller size and inaccessibility. The final classification of portosystemic shunts is determined by the branching, i.e. whether it is a single or multiple shunt system. For the purposes of this research, only the single extrahepatic portosystemic shunts will be dealt with, which are the most common type of portosystemic shunts.

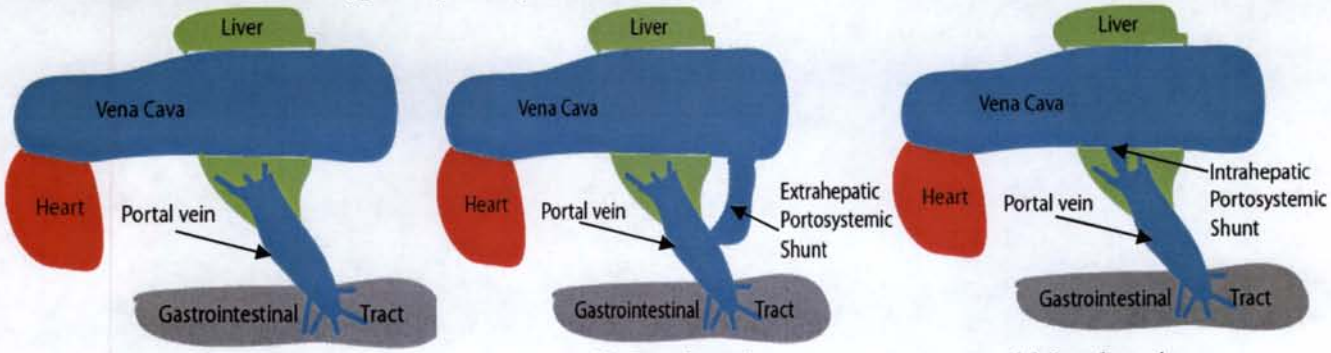

Figure 1.
(a) Normal Liver
(b) Extrahepatic Portosystemic Shunt
(c) Intrahepatic Portosystemic Shunt

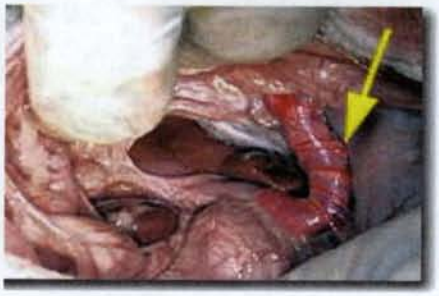

Figure 2. Image of an extrahepatic portosystemic shunt.

To understand the nature of congenital portosystemic shunts, one must first understand their formation. Fetal development begins with formation of the zygote. Pregnancy is divided into three periods: the germinal period, the embryonic period and the fetal period. After fertilization, the blastocyst begins separation in to the three main layers: endoderm, mesoderm, and ectoderm. The circulatory system develops out of the mesoderm layer. During the germinal period, the basic structure of the mesoderm layer begins to form. Next, the embryonic period marks the stage of organ development on a broad scale. Because the organs are not fully developed, organ systems such as the circulatory system are not capable of supporting the other organ systems through their own faculty. Thus, the other developing organ systems rely on the mother's circulatory system to provide the necessary nutrients and nourishment for growth. During this stage, shunts such as the ductus venosus, or the main extrahepatic portosystemic shunt form to allow the flow of blood to bypass the developing organs. At this point in the fetal development, the organ systems that are within the fetus cannot fully operate, and consequently, the fetus is dependent upon the mother's working organs. Shunts provide a way of directing blood away from dysfunctional organs. Such is the case in this situation. The mother's blood flows through the fetus via the umbilical chord, because at this stage in development the heart and liver are not fully functional. Therefore, these

shunts are necessary in delivering blood to the fetus that has been filtered by the properly working organs of the mother. During the fetal period, the organs more fully develop, and the fetus becomes less dependent upon the mother's organs. During the final portion of this period, these shunts degrade to allow the fetus to rely upon its own body functions independently of the mother.

In the past, there have been vast improvements in the approaches used to occlude these extrahepatic shunts. In the early 1990's, surgical ligation was the recommended treatment for congenital portosystemic shunts [19]. However, this simple technique has many setbacks. Mortality rates for this treatment reached percentages as high as 21% [19]. Complications due to this treatment included portal hypertension, anesthetic complications, portal vein thrombosis, or status epilepticus [19]. As a result, surgical ligation was quickly shown to be a poor treatment for this abnormality, and it was suggested that a more gradual approach to occlusion would better benefit the dog by allowing more time for the body to adjust to occlusion. For example, a slower and gradual occlusion would not have the immediate change in pressure upon the portal vein as the shunt, a major flow outlet, is closed. Establishing a slower pressure change is the main goal of this type of treatment.

The most effective treatment to date for gradual occlusion was done using an ameroid constrictor. "Ameroid is hygroscopic, compressed casein that expands when immersed in fluid. Early, rapid expansion during the first 14 days after implantation is followed by 2 months of slow expansion" [19]. The occluder was incased by a stainless steel cuff to withhold the stresses related to the expansion, as shown in Figure 3. The inner diameter is 5 mm. The shunts may vary in size from 4 mm to 1 cm, however, with

this particular procedure, gas sterilized cellophane strips were used as a partial occlusion technique initially [17]. Some occlusion is necessary at the onset in order to increase the survival chances of the dog. The locking mechanism for the device was a circular peg roughly 2 mm in diameter to allow for the insertion of the shunt. An example of the ameroid occluder in a surgical operation is shown in Figure 4. The ameroid's swelling capabilities would facilitate a tight fit between the ameroid and the lock. Results from experiments using the occluder showed 14 percent of the dogs died in the early postoperative period of portal hypertension [19]. In comparison to the surgical ligation technique, there was a suitable decrease in mortality. However, portal hypertension is still a significant issue with this technique, which is related to the majority of the swelling occurring within the first two weeks after implantation.

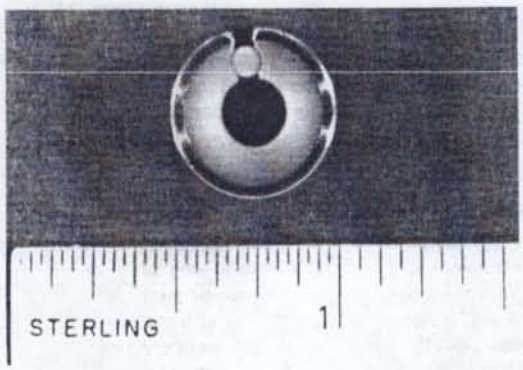

Figure 3. The ameroid occluder shown with ruler.

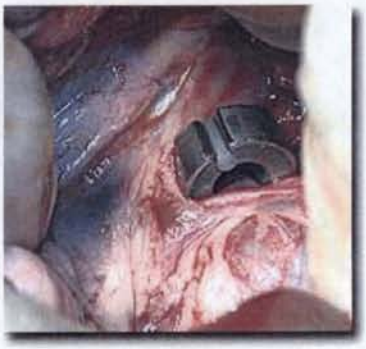

Figure 4. Ameroid occluder in surgical procedure.

Although the previous techniques have shown some promise in helping occlude portosystemic shunts, there are still complications due to the pressure changes that occur relatively quickly after treatment. Therefore, a three-month, linear occlusion technique would allow more time to adjust to the pressure changes caused by occlusion and be an ideal solution to repairing extrahepatic portosystemic shunts.

Design Analysis and Alternatives

In order to improve the design of vessel constrictors, the current design must first be studied. The current design incorporates a stainless steel outer ring, with an inner ring of ameroid, which is compressed casein. The design has an opening in the ring to allow the device to be slipped around the vessel. Once around the vessel, a rod made of casein is inserted into the opening. Upon exposure to water, the casein swells to occlude the vessel. The locking rod also swells and snugly locks the mechanism into place. Currently, the casein takes about one month to swell to completion. Previous studies have found that ameroid constrictors "undergo an initial 14 day period of rapid expansion, followed by 2 months of more gradual expansion" [1]. Further, the current design has been reported to fully occlude the vessel as quickly as 7 to 10 days and as slowly as 3 to 9 weeks [21]. Other previous studies have noted that the vessel is only 36% occluded after a six-week period [1]. Clearly, there is a discrepancy between different studies. Often, the constrictors cause enough occlusion to form a thrombus, and thus occlude the remainder of the vessel via thrombus formation. According to one study, 36% occlusion was not considered enough to result in thrombus formation.

The vessels on which the constrictors are used are typically 4mm in diameter. The constrictors are designed so that the interior diameter of the constrictor is larger than the shunt. According to Dr. Tobias, the Doctor of Veterinary Medicine with whom the authors are collaborating, the most common constrictor size used is 5 mm in diameter. Less common that this diameter are the 6 mm and 9/10 mm diameter sizes. Finally, the use of the device as a permanent implant will make it necessary for the new design of the device to be developed accordingly.

Given the current design and its limitations, improving the design is a necessity in order to improve the function of the device so that the device fully occludes the shunt. As previously mentioned, the current constrictor occludes too quickly and an improvement is needed so that the occlusion rate is linear and the occlusion time is approximately three months. The target occlusion time of three months is chosen in order to reduce the risk of complications such as hypertension and the angiogenesis of new shunts. Another problem is that the opening to slide the constrictor around the vessel is sometimes not large enough. If the vessel is large, it must be collapsed in order to slide the ring around it. If the vessel is too large, often the surgeons resort to surgical ligation of the shunt instead of a constrictor. Last, and most important, the unreliability of the current constrictor produces the need for a reliable method for occluding shunts.

The first step in the design process was to choose a method of occlusion that would take about three months to fully occlude the vessel. The possibility of using a hydrogel was considered first. After researching the idea, it was decided that this approach was not feasible given the time constraints. There are currently no hydrogels that are commercially available that have a swelling rate slow enough to accommodate a

three-month swelling period. Indeed, such a hydrogel could be synthesized, but finding the correct polymers to copolymerize and the correct percentages of each polymer needed merits a Ph.D. thesis.

The next idea to be considered was the improvement of the swelling rate of the ameroid. Previous studies were conducted where the ameroid was coated with petrolatum in order to try to slow the swelling rate, but the results showed this method lacking [1]. The idea was to coat the ameroid with a biocompatible metal or with carbon as opposed to petrolatum. The ameroid would be coated in such a way that there would be regions of non-coated ameroid between the metal or carbon coating to allow water to enter at a slower rate, thus slowing the expansion of the ameroid. The coating material would be evaporated and sputtered on the ameroid through a mask, which would allow for the non-coated regions. A depiction of this process is below in Figure 5.

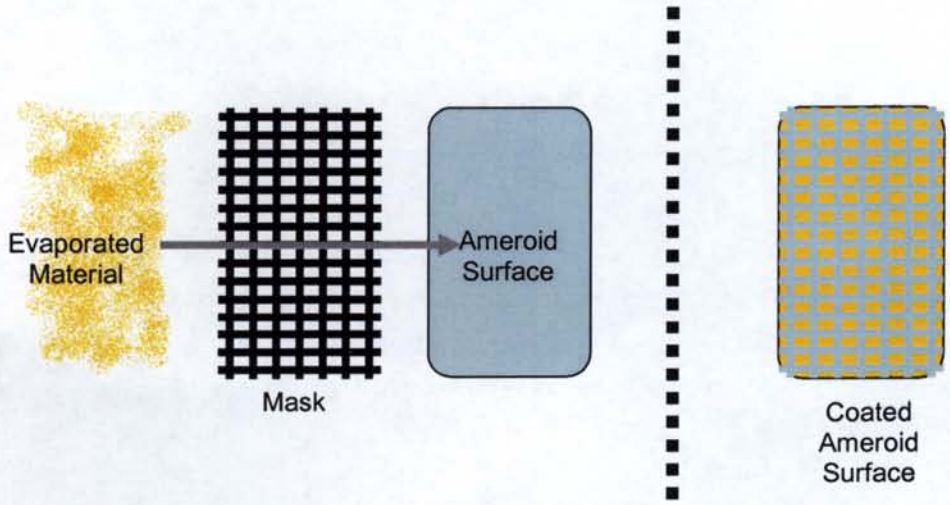

Figure 5. Depiction of masking the ameroid surface.

The mask, which looks similar to a screen window, would be placed over the ameroid surface, and then the evaporated coating would be applied to the ameroid and allowed to set. The fineness of the mask, i.e. how much ameroid surface area the mask allows to be

coated, would determine the swelling rate. Masks of different fineness would then be tested to determine the surface area of coating needed to obtain the desired swelling rate and thus occlusion time. This idea was abandoned, however, for a couple of reasons. The first reason is that the idea lacks significant improvement over the current design. While it may indeed swell at a slower rate, there is still the likelihood that most of the swelling will occur in the first two weeks instead of a more constant, linear swelling rate. Second, problems may have arisen in trying to get the evaporated material to adhere to the ameroid. Also, the current inability of the ameroid to fully occlude the vessel is not resolved with this method. Finally, we felt that this idea was too similar to the current idea, and wanted to come up with a better, more innovative idea.

The final idea explored for the occlusion method was to create a more mechanically-based constrictor. This idea was adopted and, after much debate and discussion, a design selected. The chosen design needed to, as aforementioned, consistently and completely occlude a vessel at a constant rate for a three-month period. In order to mechanically occlude a vessel, the device must be able to apply a force that increases, with respect to time, and eventually becomes large enough to collapse the vessel. In essence, some type of spring-loaded system would be needed to consistently apply these sorts of forces. The spring-loaded system was the first design iteration, and was abandoned later due to the size of the device. Next, a decision was made to use a hydrogel placed in a pressure plate to achieve the spring compressive force needed. A biodegradable polymer is used to resist the compressive forces of the hydrogel. As the polymer degrades, the hydrogel will slowly occlude the shunt. Thus, the rate and linearity of occlusion is dependent on the biodegradable polymer selection. The force

provided by the hydrogel will actually remain relatively constant after its initial swelling, rather than increasing with time, but will be prevented from quickly occluding the shunt by the biodegradable polymers.

First, the forces needed to occlude the shunt had to be considered. The typical venous pressure in hepatic portal shunts in dogs is between 4 and 8 mm Hg. Sometimes the pressure will be as high as 10 mm Hg and rarely as high as 12 mm Hg. Thus, the hydrogel must be able to overcome these pressures in order to occlude the shunt. In order to be certain that the shunt will become fully occluded, the target hydrogel force should be a few times larger than the maximum possible venous pressure. Thus, the target pressure to be provided by the hydrogel is 15 mm Hg. This is still a very small pressure. This pressure can be translated into a force by the equation given below,

$$F = P \times A$$

Equation 1.

where F is the force, P is the venous blood pressure, and A is the surface area in contact with the occluder pressure plate. The actual force needed from the hydrogel will be delineated later.

Then, the exterior design of the occluder was addressed. Several ideas were considered including a spherical exterior, a cylindrical exterior, and a ring exterior. In the first iteration design, a ring exterior was used because it allows the most contact with body fluids. Additionally, the ring exterior requires the least amount of material thus reducing the weight of the device. Consideration of the fabrication of the device indicated that a ring exterior would be too difficult to machine given the overall size of the device. Furthermore, a ring exterior would not have prevented the hydrogel from

seeping out of the pressure plate. Thus, the design was modified to make a rectangular exterior (See Appendices).

Next, a decision needed to be made on how to incorporate the biodegradable polymer in such a way that would allow the hydrogel to expand and occlude the shunt. Simultaneously, the best way to control the degradation rate had to be considered as the degradation rate can be affected by the placement of the polymer. Based on the concept of the design, the biodegrading polymer should be placed on either side of the vessel in order to achieve uniform occlusion. Fortunately, biodegradable polymers are widely commercially available and several have degradation rates that are approximately three months or much longer than three months. Furthermore, the shape of the biodegrading polymer must be considered. The polymer needs to be in a shape in which degradation causes a reduction in size in the direction of loading of the vessel. This can be challenging when using surface-eroding polymers (which is the type of eroding polymer selected as will be discussed in the materials section) because any surface that is in contact with another surface on the device will not be exposed to the body fluids and thus will not degrade. For example, if a rectangular shape were chosen for the biodegrading polymer, the vertical sides of the polymer would degrade to the point where the hyrdogel forces would cause the collapse of the polymer and instantaneous occlusion of the shunt (See Figure 6). This would defeat the purpose of the design since it seeks to occlude the shunt gradually.

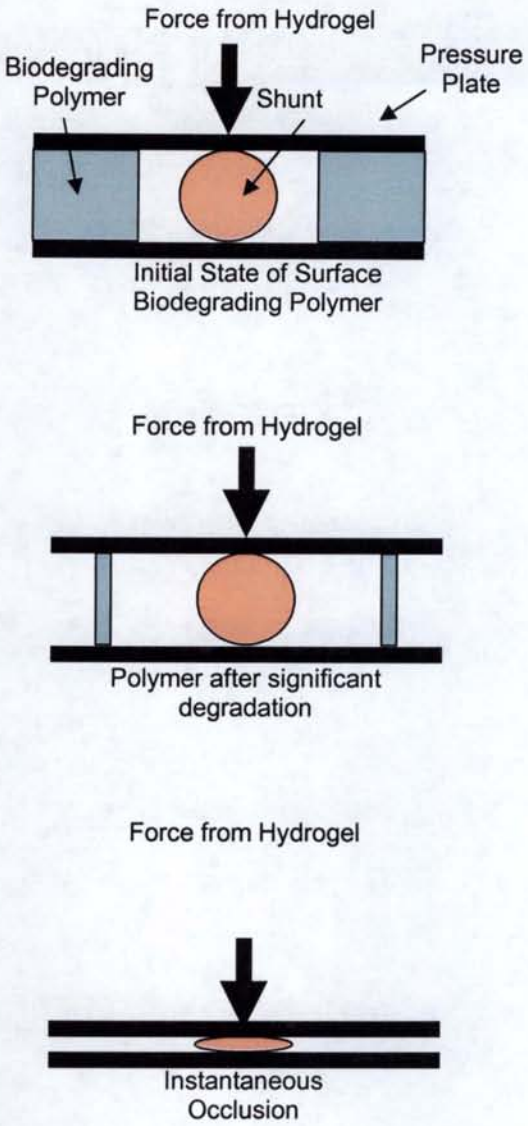

Figure 6. Illustration of a poor shape choice for the surface-eroding biodegrading polymer.

In order to attain degradation in the vertical direction, a cylindrical shape was used. This shape will only be in contact in two single points, the top and the bottom of the cylinder. Thus, most of the surface of the cylinder will be exposed to the body fluids and it should degrade uniformly in the desired direction. Using a cylindrical biodegradable polymer has its limitations in that unless secured into place, it could slide out of the device. In the first iteration design pegs were placed on the top and bottom of the cylinder that would fit into the pressure plate and the casing in order to prevent sliding from occurring.

The final aspect of the design is the locking mechanism. A mechanism is needed to lock the constrictor into place once it has been placed around the vessel. The current design is adequate and works relatively well. The main consideration for changing the lock was to use a hinge. This was decided against because a hinge introduces too many risks such as pinching and rupturing the vessel or perhaps injuring surrounding tissues and organs if shifted after implantation. Furthermore, our device is so small that implementing a hinge into the design would be nearly impossible. Thus, the current locking mechanism employed by the ameroid occluders was deemed sufficient, but perhaps the shape could be modified to allow more room for the vessel to enter and to better keep the lock in place until it has had time to swell shut. A counterlocking mechanism was considered which would secure the lock into place by a method other than swelling.

After considering all of the above ideas, developing preliminary and first iteration designs, a second iteration design was developed that still incorporates a drawer held open by a biodegradable polymer. The drawer, or occluder pressure plate, is simply an open-lid-box design that is held in contact to the degradable polymer by a compression force. Figure 7. and Appendix I-A show illustrations and layouts of the pressure plate. The open box would have dimensions 12.5 mm by 5.5 mm by 2 mm, with a thickness of 0.5 mm around the sides and a thickness of 1.0 mm along the base. The hyrdogel was designed to fit into the drawer with the dimensions 11.5 mm by 4.5 mm by 1mm. As the hydrogel swells due to water absorption, it will cause a compressive force between the casing and the drawer. The casing is fitted with holes in the top layer to allow for body

fluid contact with the hydrogel. Illustrations of the hydrogel can be found in Figure 8 and Appendix B.

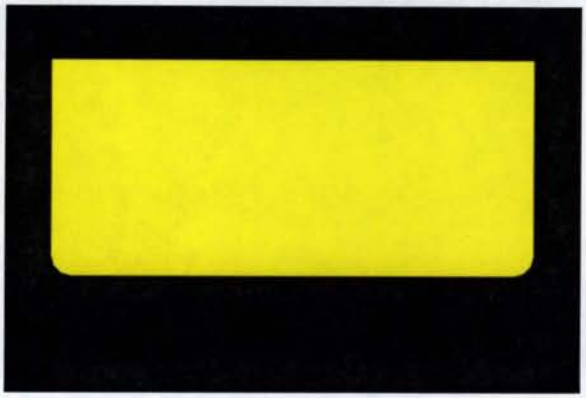

Figure 7. Occluder Pressure Plater.

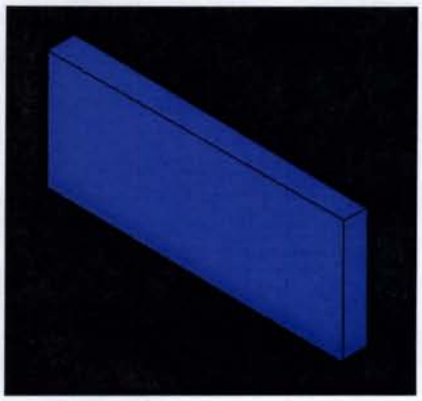

Figure 8. Hydrogel.

Furthermore, the force needed from the hydrogel was calculated so that appropriate considerations for material selection would be available. Since the depth of the pressure plate is 1 mm, we can assume that the plate will be in contact with a 1 mm length of the vein. The diameter of the vein is 4 mm, thus we can estimate the surface area of vein in contact with the plate as a rectangle that is 4 mm in length and 1 mm wide and area 4 mm^2.

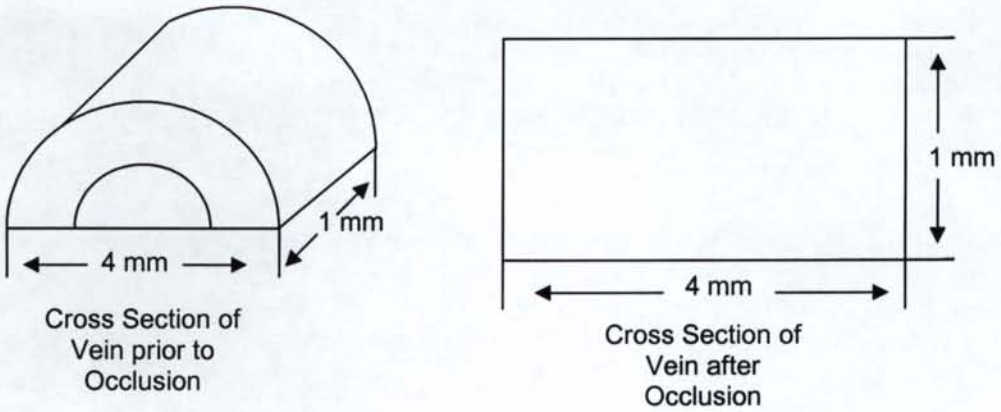

Figure 9. Illustration of surface area estimation used for force calculation.

This is an accurate assumption since this will be the approximate surface area in contact when the vessel is fully occluded. Thus, the hydrogel must be able to achieve this maximum force and maintain it even though the pressure in the shunt may decrease once it is fully occluded. The needed force then is (from Equation 1.)

$$4\ mm^2 \times 15\ mm\ Hg \times \frac{133.28\ (N/m^2)}{1\ mm\ Hg} \times \frac{1\ m^2}{(1000\ mm)^2} = 0.0019992\ N = 1.9992\ mN$$

As a surface eroding biodegradable polymer was chosen as the degrading polymer, it was essential to ensure that the surface would erode in a uniform manner. As aforementioned, structures such as cubes and pyramids were considered until the cylindrical shape was finally decided upon for reasons previously discussed. Due to the possibility that the polymer structure could slide out from under the plate, there had to be some mechanism to hold the polymer in place. Small 1 mm by 1 mm by 4 mm fins were considered for the second iteration design, however, we found them to be extremely difficult to machine. For this reason, the fins were abandoned (shown in Appendix II-C). Instead, a modified version of our original design was reverted to which has pegs that extend out of the bottom of the cylinder and fit into holes in the casing to prevent the polymer from sliding out of the device and allow for stability during degradation. Because the pegs, though made of biodegradable polymer, theoretically should not be exposed to the body fluids, they should hold their mechanical properties until the entire degradable polymer erodes. An illustration of the biodegradable polymer may be found in Figure 10 and Appendix I-C. Because the estimated shunt diameter once partially occluded by the cellophane wrapping is 4 mm in diameter, the biodegradable polymer at first must also be 4 mm in diameter. For support, the peg inserts were 1 mm in diameter and extend 1 mm beyond the tangent point of the cylinder.

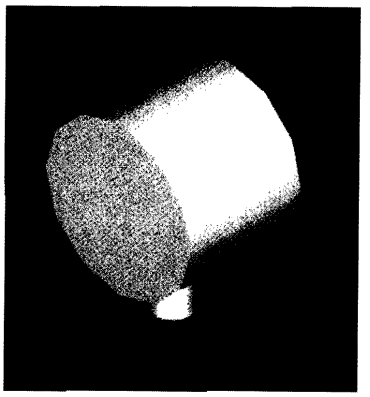

Figure 10. Biodegradable polymer.

Of all of the structural pieces of the design, the most complex design was the casing. Because the casing had to have an entrance way for the vessel, the casing could not be one complete piece, but a combination of pieces. In the first rectangular design, the design consisted of a two piece system of an outer casing that surrounded the occluder plate and was completed with a hexagon lock. Each side of the hexagon was 2 mm with a 4 mm thickness of the piece. An illustration of this piece may be seen in Appendix II-A. However, due to machinability factors, the hexagon was substituted with an easier machinable circular piece with sections removed to allow for a flat surface to eventually come into contact with the occluder pressure plate. Figure 11 shows the image of the cylindrical lock, as well as Appendix I- D. The diameter, 4.4721 mm, of the cylinder was calculated to allow for a 2 mm entrance space for the shunt. In addition, between the two flat surfaces there is a 4 mm distance, which is equivalent to the distance on the casing. To prevent the lock from spinning or sliding out, a rod is inserted through the side of the cylinder as a counterlock to ensure proper placement. The 1 mm diameter hole can be seen in Figure 11 also. The rod's dimensions are 0.9 mm in diameter by 10

mm in length. The rod needs to fit snugly into the hole to ensure that it does not slip out of the casing, and holds the lock in place. Figure 12 and Appendix I- E display the rod's structure.

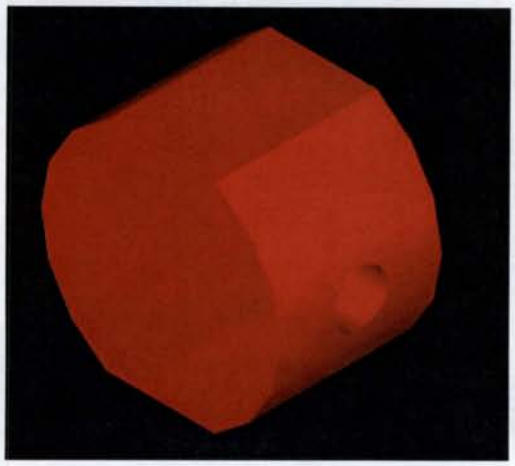

Figure 11. Cylindrical Lock.

Figure 12. Locking Rod.

Another complication occurred in the design with the inability to insert the pressure plate into the casing after machining. Therefore, another piece was cut out as a top to allow for the insertion of the occluder plate and the hydrogel. Therefore, the casing design changed from the single top as shown in Appendix II-B to the combination of the top, two screws and the casing as shown in Appendix I- F, G, and H respectively. The occluder top is 16.5 mm by 2 mm by 3 mm. In addition, the occluder top can also be found in Figure 13, which shows the two outer holes spaced 1 mm from the shorter edges and 1.5 mm to the longer edges from the center of the 1 mm diameter circle. These holes provide an entry for the screws that will hold the top together with the casing. The screws, shown in Figure 14., will be able to withstand the pressure exerted by the hydrogel. Furthermore, there are three holes, 2 located 5 mm from the shorter side of the

top and 1.5 mm from the longer side and 1 in the very center, all 1 mm in diameter. As Appendix I- F will show, these holes extend all the way through the top's 2 mm thickness. These three holes allow for body fluid contact with the hydrogel initiating the expansion process of the hydrogel. Without these holes, the compressive force of the hydrogel would not be nearly as great.

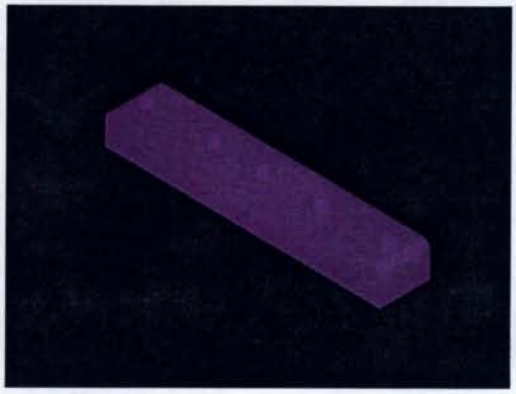

Figure 13. Occluder Top.

Finally, the casing is the sum of the leftover space in need of support. The overall dimensions of the casing are 16.5 mm by 13.5 mm by 3 mm. Extending from the top of the casing is a 14.5 mm by 5.5 mm by 2 mm hole to allow for the pressure plate to be inserted. Along the top are two 1 mm diameter holes that are 1.0 mm from the shorter side and 1.5 mm from the longer side and 1 mm deep to line up with the occluder top. These holes are necessary for the screw insertion. Below the pressure plate space is a 14.5 mm by 4 mm by 3 mm space for two biodegradable polymers to be inserted. 2 mm from either inner wall are 1 mm diameter and 1 mm deep cylindrical cut outs to match the pegs protruding from the biodegradable polymer structures. Furthermore, there is a space for the cylindrical lock, with a diameter of 4.4721 mm and 3 mm deep.

Moreover, there is a 1 mm diameter and 10 mm cylindrical cut out extending through one side of the casing. The hole is centered 2 mm up from the bottom on the side perpendicular to the face in the Figure 15. Diagrams of the older versions of the casing may be found in Appendix II-C, which contain the hexagon lock, complete with top and fins to hold the biodegradable polymer in place.

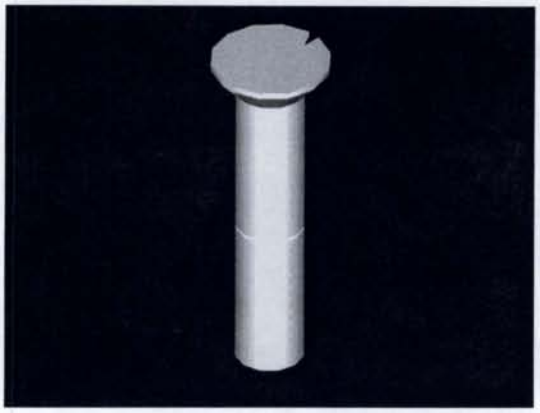

Figure 14. Countersunk Screw

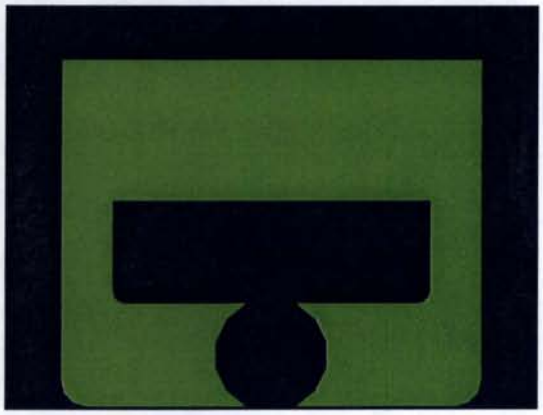

Figure 15. Occluder Casing.

In conclusion, each piece of the design was selected without regard to the material with which it was to be made. The material properties of each material were investigated separately to match and enhance the features of the design. After conducting a patent search, the above design is was found to be novel and completely original. An image of the completely assembled design can be seen in Figure 16 (a) and (b) as well as Appendix I-I.

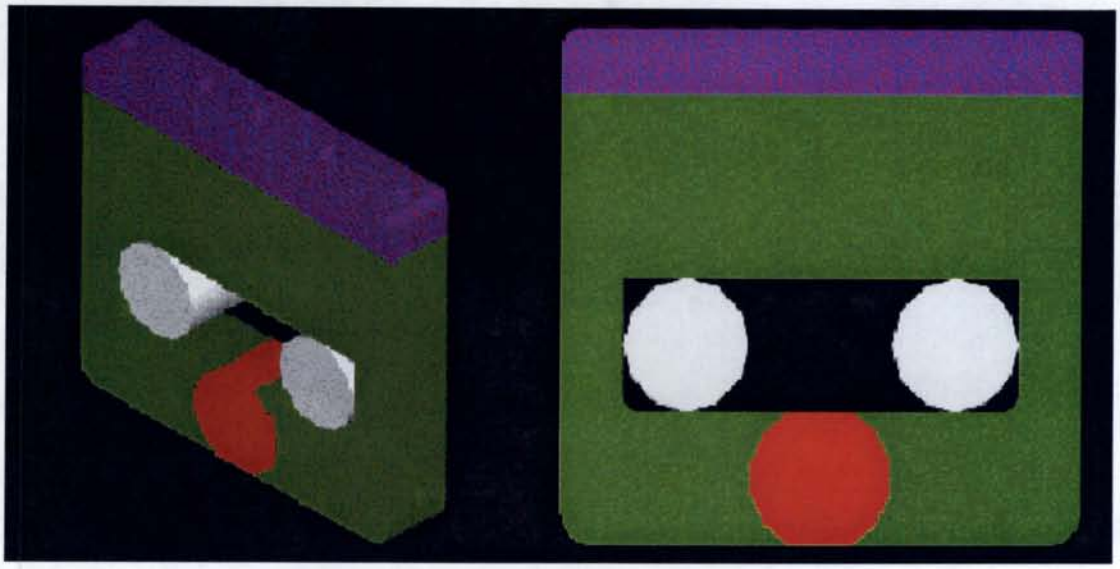

Figure 16. (a) Orthogonal view of the complete occluder and (b) front view of complete occluder.

Materials and Methods

In an attempt to maintain a fluid paper, we consider each material separately in its entirety.

Ultra-High Molecular-Weight Polyethylene

Specifications

The material used for the casing needs to be mechanically sturdy yet light. Since the pressure and forces to be exerted are small, the material does not necessarily have to have extreme mechanical properties. The chosen material does need to maintain its structural integrity throughout the life of the dog despite the aqueous environment in which it will be surrounded. The chosen material must also have well-established biocompatibility in order to ensure the safety of the dog. Furthermore, the material should be resistant to cell adhesion as this might impede the function of the device by

blocking the occluder pressure plate or by encapsulating the device. Since this material will also be used for the occluder pressure plate, it needs to be smooth enough so as not to create enough friction to prevent the device from occluding the shunt.

Material

Ultra-high-molecular-weight polyethylene (UHMWPE) was selected as the polymer to be used for the casing, lid, occluder pressure plate, circular lock, and rod lock. UHMWPE has well-established and well-documented biocompatibility. Furthermore, UHMWPE has a Young's Modulus that is approximately 20 MPa, which greatly exceeds any of the forces that will be present in the device. UHMWPE is renowned for the inability of other materials to adhere to its surface. Thus, UHMWE will be resistant to the aforementioned cell adhesion that might occur *in vivo*. Finally, UHMWPE is much lighter than the stainless steel used in the ameroid ring constrictors.

Method of Machining

UHMWPE was easily obtained from the materials science department. The UHMWPE was then machined into our design in the machine shop in the basement of Dougherty. Doug Fielden did all of the machining necessary to create the pieces of the device.

Testing and Results

The device was not finished until the last week of the semester. Due to this fact, and other problems that arose, the device was not able to be tested. Hence there are no

results to report. The mechanical properties of UHMWPE were not tested because they are well-known and nothing experimental was done to the UHMWPE that would arouse suspicion that its properties might have changed.

Discussion

As there are no results, there is not much to discuss. UHMWPE is an ideal material for a device such as this. UHMWPE has very good mechanical properties, biocompatibility, resistance to adhesion, and is one of the more easily machined plastics. UHMWPE is also much lighter than the stainless that was used in the previous device. Thus, UHMWPE is an excellent choice.

PVA Hydrogel

Specifications

The material used in the occluder pressure plate of the device needs to have four main characteristics. First, the material must exert the force needed to overcome the venous pressure of the shunt. Second, the material must have a high swell ratio compared to its initial size. Third, there must be an instantaneous swell to maintain positioning of the other parts of the device. Finally, minimal degradation must take place to ensure the integrity of the material.

The venous pressure of the shunt in an average dog ranges from 4-8 mmHg. If the dog is stressed, the venous pressure can increase to 10 mmHg. The material in the occluder pressure plate, therefore, must be able to overcome this pressure to occlude the

shunt completely. The force applied by the material will induce force onto the occluder pressure plate, which will then exert a force onto the shunt itself.

The occluder pressure plate has dimension of 11.5 mm x 4.5 mm x 1 mm and the material must initially fill this volume and then swell as the biodegradable polymer below the occluder pressure plate degrades and the shunt is occluded. The estimated swelling ratio needed to close the occluder without any opposing pressure is 2.125X, but when the vein is present, the swelling ratio will need to be larger to overcome the venous pressure. Thus we estimate needing a swelling ratio that is 7-8X its initial size. This will ensure that the hydrogel will overcome the venous pressure. Additionally, if the material degrades, the remaining material will have enough swelling to maintain the force needed.

The swelling of the material must occur instantaneously to hold all parts of the device in the proper positions. The biodegradable polymer will be held in by small pegs and the shunt by a lock mechanism on the device, but the extra force from the swelling will help ensure that these parts maintain their proper position. A range of instantaneous to a few hours post-insertion is optimal.

The force from the occluder pressure plate needs to be constant and reach equilibrium within the first 24 hours and maintain this force through the duration of the occlusion. This force must also be fairly constant throughout the dog's life because the device is intended to be permanent. Therefore, the material must have minimal degradation to prevent a decrease in water uptake, which in turn will decrease the swelling and the amount of force applied.

Material

A polyvinyl alcohol hydrogel (PVA-H) was selected as the hydrogel material. Hydrogels are cross-linked polymers that form a scaffold that uptakes water and consequently swells. Cellular freeze/thawed PVA-H was chosen over chemically cross-linked PVA-H due to the greater mechanical strength of the cellular freeze/thawed PVA-H. Within the PVA-H, crystalline regions operate as physical crosslinks, caused by hydrogen bonding, to provide this enhanced mechanical strength. These regions serve to better dissipate the mechanical load or stress. In addition, the freeze/thawed PVA-H has demonstrated a higher elasticity and can sustain an extension of up to six times its initial length. The swelling ratio of PVA-H has been shown to reach a maximum of 8X its initial volume from a dry state and reach an equilibrium swelling at approximately 6X its initial volume [5]. PVA-H has also been proven to have excellent biocompatibility and durability. In addition, by varying the amount of water content, the viscoelastic properties can be controlled [6].

Method of Synthesis

Protocol from previous literature [5] was used as a basis for the synthesis. A ten percent weight amount of poly vinyl alcohol was dissolved in deionized water. The process to perform this portion was not specified in the previous protocol. The PVA (97% hydrolyzed, MW= 50,000 – 85,000 g/mol) was dissolved through refluxing at 90 degrees Celsius for 6 hours in an oil bath. A stir bar was added to assist in the dissolving process. Following the six hour heating, the PVA solution was poured into either a PE or a PTFE mold and stored in a glass dessicator filled with Drierite (compared to the

previous protocol, which cast the solution onto microscope slides) and frozen at a range between -15 and -20 degrees Celsius. Drierite was used to prevent excess absorption of water from the atmosphere. The PVA suspension remained in the freezer for 8 hours. After which, the PVA was removed from the freezer and allowed to thaw for 4 hours. This freeze and thaw cycle was repeated two more times to complete a total of three freeze-thaw cycles.

The synthesis of PVA-H proved to be more difficult than first expected. The initial attempt at synthesis heated the PVA into solution in an oven and then the freeze/ thaw process was performed. This synthesis produced an uneven hydrogel that consisted of three layers with the bottom layer crystalline hydrogel, the middle layer a semi-crystaline hydrogel, and the top layer a liquid. The entire synthesis was carried out in a glass beaker, which was sealed in an airtight bag with Drierite during the freeze/thaw process. In the second attempt, a stir bar was added to ensure complete dissolution of the PVA into the deionized water. In addition, this synthesis was performed in a hood to prevent water from the atmosphere from entering the solution. As a result of being in the hood, the boiling point of the water was lowered and the temperature of 90°C caused the water to boil off. The third attempt utilized the same method as the second, only it was monitored to add water as needed into the solution, but the water boiled off within minutes of reaching 90°C. Neither the second nor third attempts were put through the freeze/thaw process. The fourth attempt was refluxed using a water bath to heat the solution. Water from the water bath boiled off and when this occurred more water was added. The addition of water resulted in a drop in temperature of the water bath. Finally,

the oil bath was used to prevent boiling off and to maintain a constant temperature at 90°C.

Testing and Results

To verify that the PVA-H was crosslinked, we did a number of tests to measure the swelling ratio of the resulting hydrogel. Swelling ratio was determined by the equations given below,

$$Swelling\ RatioX = \frac{m_f}{m_0}$$

$$Swelling\ Ratio\ \% = \frac{m_f}{m_0} \times 100$$

Equations 2 and 3.

where m_0 is the initial mass, and m_f is the final mass or mass calculated at every measurement hour. The swelling rate was determined by the following equation,

$$SwellingRate = \frac{\partial m}{\partial t}$$

Equation 4.

The initial tests were performed in deionized water at a temperature of 25°C. Two tests were performed simultaneously. The initial masses were 1.29 grams (sample 1) and 0.572 grams (sample 2). For the first six hours, mass measurements were taken once an hour. At 24, 48 and 72 hours, mass measurements were taken to observe the swelling ratio over a period of three days. The swelling ratios hit maxima at approximately 24 hours (sample 1) and between 6-24 hours (sample 2). Sample 1 swelled to 2X its initial size and sample 2 to 2.5X its initial size. Swelling increased until

hour 24, then began to decrease slightly in sample 1. Decrease in the rate of swelling began at hour 24.

Hour	Mass (grams)	Swelling Ratio X	Swelling Ratio %	Swelling Rate
0	1.29	1	100	0
1	1.79	1.387596899	138.7596899	0.5
2	1.944	1.506976744	150.6976744	0.154
3	2.12	1.643410853	164.3410853	0.176
4	2.27	1.759689922	175.9689922	0.15
5	2.39	1.852713178	185.2713178	0.12
6	2.45	1.899224806	189.9224806	0.06
24	2.688	2.08372093	208.372093	0.013222222
48	2.5044	1.941395349	194.1395349	-0.00765
72	2.343	1.81627907	181.627907	-0.006725

Table 1. PVA-H Test 1 in Deionized Water at 25°C—Sample 1.

Hour	Mass (grams)	Swelling Ratio X	Swelling Ratio %	Swelling Rate
0	0.572	1	100	
1	0.868	1.517482517	151.7482517	0.296
2	1.056	1.846153846	184.6153846	0.188
3	1.23	2.15034965	215.034965	0.174
4	1.32	2.307692308	230.7692308	0.09
5	1.385	2.421328671	242.1328671	0.065
6	1.45	2.534965035	253.4965035	0.065
24	1.4215	2.48513986	248.513986	-0.001583333
48	1.33	2.325174825	232.5174825	-0.0038125
72	1.273	2.225524476	222.5524476	-0.002375

Table 2. PVA-H Test 1 in Deionized Water at 25°C—Sample 2.

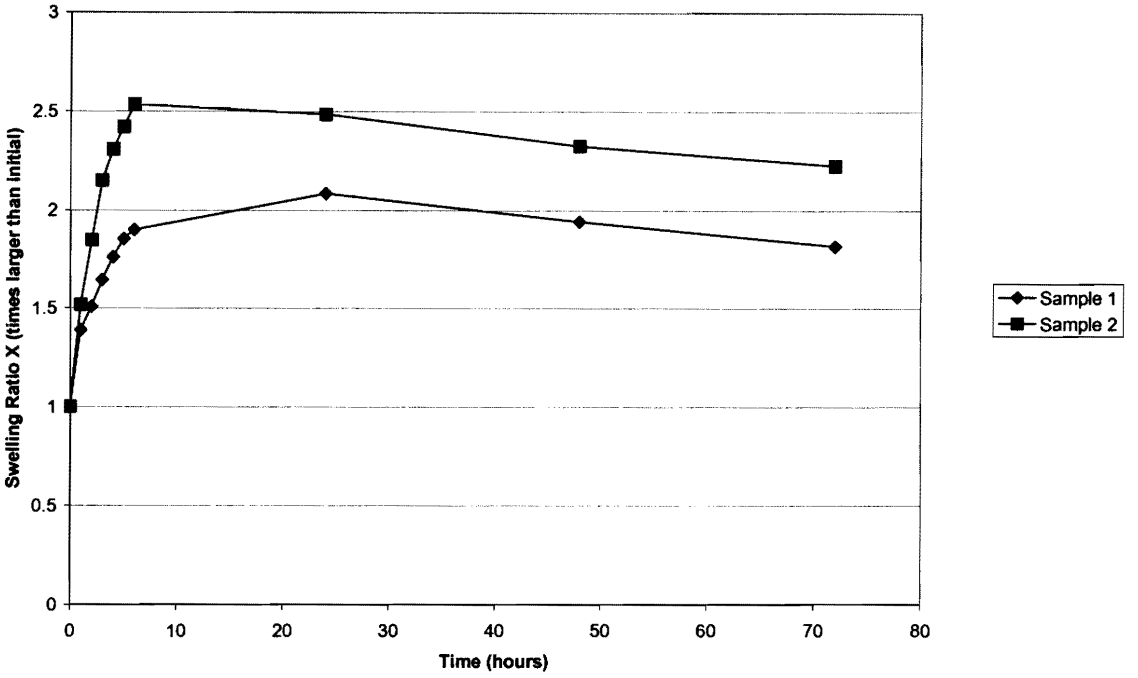

Figure 17. Swelling Ratio of PVA-H Versus Time in Deionized Water at 25°C.

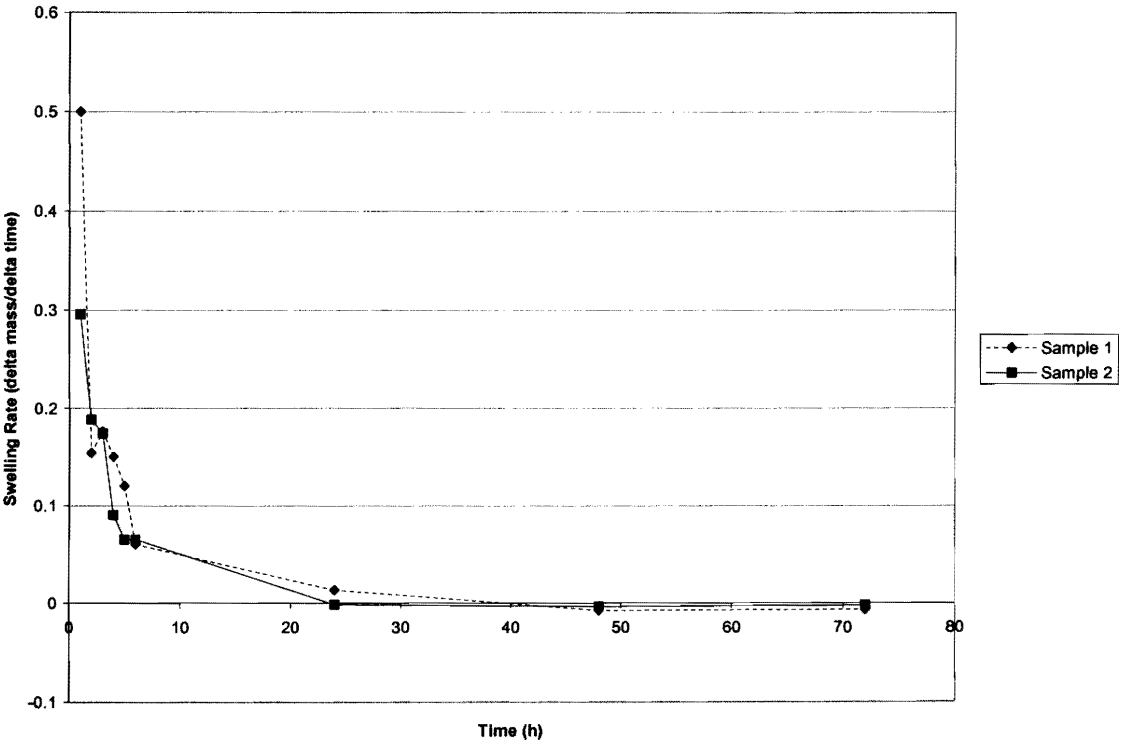

Figure 18. Swelling Rate of PVA-H Versus Time in Deionized Water at 25°C.

The second tests were performed in deionized water at a temperature of 37°C similar to those previously performed [5]. Three samples were tested simultaneously. The initial masses were 0.1076 grams (sample 3), 0.102 grams (sample 4), and 0.0928 grams (sample 5). For the first five hours, mass measurements were taken once an hour. At 24 hours, a final mass measurement was taken. At the fifth hour, the samples began to degrade and further testing became more difficult. Samples 3 and 4 reached maximum swelling at hour 4 and sample 5 reached maximum swelling at hour 5. Sample 3 swelled to over 2.8X, sample 4 over 2.3X, and sample 5 over 2.1X their initial sizes. Decrease of swell rate began at the fourth hour for sample 3 and the fifth hour for sample 4. Sample 5 experienced a decrease at the third hour, but increased again at the fourth hour. Decreased swell rate occurred again at hour 24.

Hour	Mass (grams)	Swelling Ratio X	Swelling Ratio %	Swelling Rate
0	0.1076	1	100	
1	0.234	2.17472119	217.472119	0.1264
2	0.2845	2.644052045	264.4052045	0.0505
3	0.3046	2.830855019	283.0855019	0.0201
4	0.3032	2.817843866	281.7843866	-0.0014
5	0.2895	2.690520446	269.0520446	-0.0137
24	0.2098	1.949814126	194.9814126	-0.004194737

Table 3. PVA-H Test 2 in Deionized Water at 37°C—Sample 3.

Hour	Mass (grams)	Swelling Ratio X	Swelling Ratio %	Swelling Rate
0	0.102	1	100	
1	0.1988	1.949019608	194.9019608	0.0968
2	0.2269	2.224509804	222.4509804	0.0281
3	0.2326	2.280392157	228.0392157	0.0057
4	0.242	2.37254902	237.254902	0.0094
5	0.2292	2.247058824	224.7058824	-0.0128
24	0.208	2.039215686	203.9215686	-0.001115789

Table 4. PVA-H Test 2 in Deionized Water at 37°C—Sample 4.

Hour	Mass (grams)	Swelling Ratio X	Swelling Ratio %	Swelling Rate
0	0.0928	1	100	
1	0.1867	2.011853448	201.1853448	0.0939
2	0.2016	2.172413793	217.2413793	0.0149
3	0.1905	2.052801724	205.2801724	-0.0111
4	0.1926	2.075431034	207.5431034	0.0021
5	0.1968	2.120689655	212.0689655	0.0042
24	0.1879	2.024784483	202.4784483	-0.00047

Table 5. PVA-H Test 2 in Deionized Water at 37°C—Sample 5.

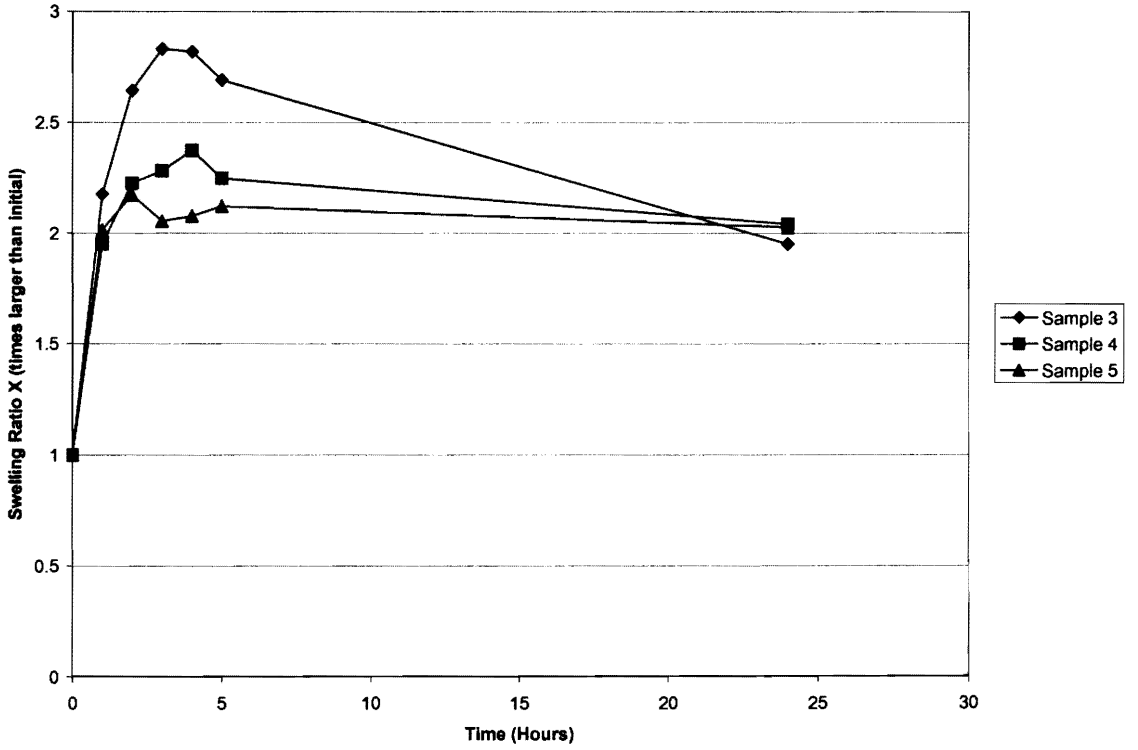

Figure 19. Swelling Ratio of PVA-H Versus Time in Deionized Water at 37°C.

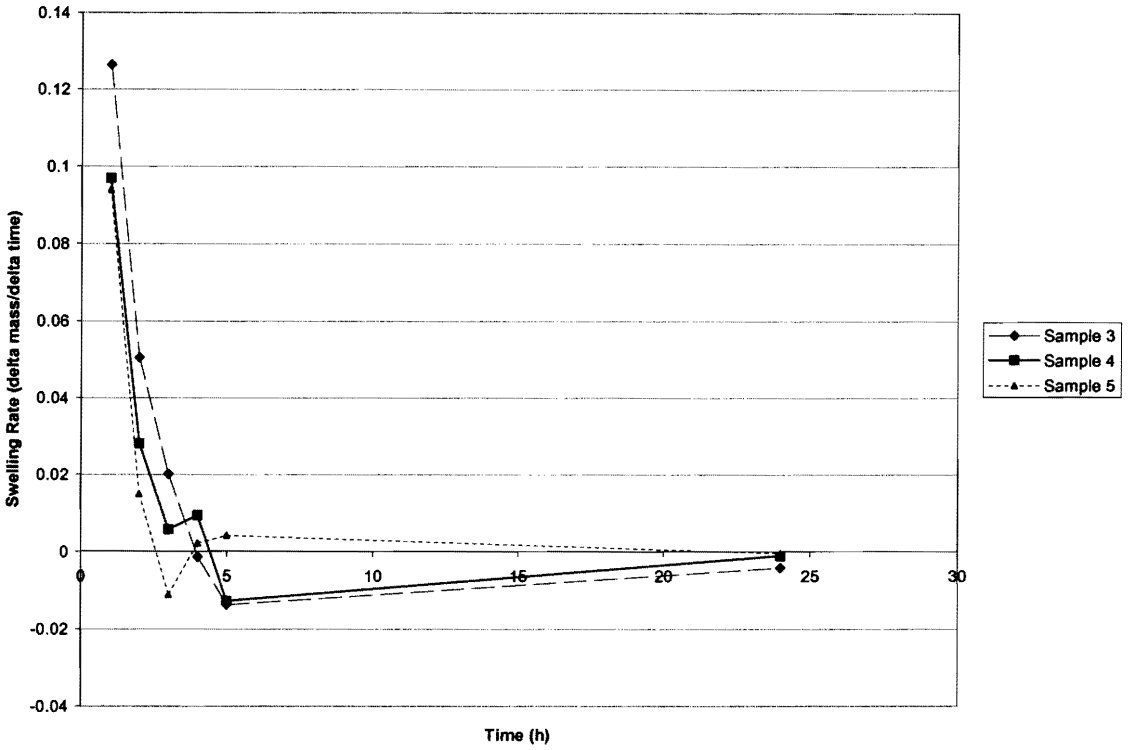

Figure 20. Swelling Rate of PVA-H Versus Time in Deionized Water at 37°C.

The third set of tests were performed in simulated body fluid at a temperature of 37°C. The simulated body fluid was made using the method described in Tas [15] outlined below.

Order	Reagent	Amount (g/L)
1	NaCl (Sodium Chloride	6.547
2	$NaHCO_3$ (Sodium Bicarbonate	2.268
3	KCl (Potassium Chloride	0.373
4	$Na_2HPO_4*2H_20$ (Sodium Phosphate Dibasic dehydrate)	0.178
5	$MgCl_2*6H_20$ (Magnesium Chloride Hexahydrate)	0.305
6	$CaCl_2*2H_20$ (Calcium Chloride Dihydrate)	0.368
7	Na_2SO_4 (Sodium Sulfate)	0.071
8	$(CH_2OH)_3CHN_2$ (Tris(hydroxymethyl)aminomethane)	6.057

Table 6. Reagents used for Simulated Body Fluid Synthesis.

The first five of the above reagents were added to 700 mL of deionized water while stirring with a magnetic stir rod. Then 15 mL of 1 M HCl was added. Next, reagents six through eight were added to the mixture while stirring. Then the solution was placed ijn a water bath at 37°C and allowed to reach that temperature. Then the solution was titrated with 1 M HCl to a pH of 7.4 while adding deionized water to bring the solution near 1 L. Then the solution was brought to exactly 1 L [15].

Three samples were tested simultaneously in the simulated body fluid. The initial masses were 0.4508 grams (sample 6), 0.4548 grams (sample 7), and 0.4596 grams (sample 8). Mass measurements were taken once an hour for the first five hours and then again at 24 hours. Measurements of sample 8 became impossible to measure after the third hour due to high degradation. Sample 6 swelled to 1.5X the initial mass at the fifth hour. Sample 7 reached a maximum swelling of over 1.6X the initial mass at the fifth hour. The decrease in swelling rate for samples 6 and 7 occurred at hour 24, whereas the decline of sample eight began in the third hour.

Hour	Mass (grams)	Swelling Ratio X	Swelling Ratio %	Swelling Rate
0	0.4508	1	100	
1	0.6646	1.474267968	147.4267968	0.2138
2	0.6692	1.48447205	148.447205	0.0046
3	0.682	1.512866016	151.2866016	0.0128
4	0.6924	1.535936114	153.5936114	0.0104
5	0.7023	1.557897072	155.7897072	0.0099
24	0.6229	1.38176575	138.176575	-0.0042

Table 7. PVA-H Test 3 in Simulated Body Fluid at 37°C—Sample 6.

Hour	Mass (grams)	Swelling Ratio X	Swelling Ratio %	Swelling Rate
0	0.4548	1	100	
1	0.6581	1.447009675	144.7009675	0.2033
2	0.6954	1.529023747	152.9023747	0.0373
3	0.7094	1.559806508	155.9806508	0.014
4	0.7499	1.64885664	164.885664	0.0405
5	0.7526	1.654793316	165.4793316	0.0027
24	0.6481	1.425021988	142.5021988	-0.0055

Table 8. PVA-H Test 3 in Simulated Body Fluid at 37°C—Sample 7.

Hour	Mass (grams)	Swelling Ratio X	Swelling Ratio %	Swelling Rate
0	0.4596	1	100	
1	0.5473	1.190818103	119.0818103	0.0877
2	0.598	1.301131419	130.1131419	0.0507
3	0.5636	1.226283725	122.6283725	-0.0344
4	threw out because sample was too damaged			

Table 9. PVA-H Test 3 in Simulated Body Fluid at 37°C—Sample 8.

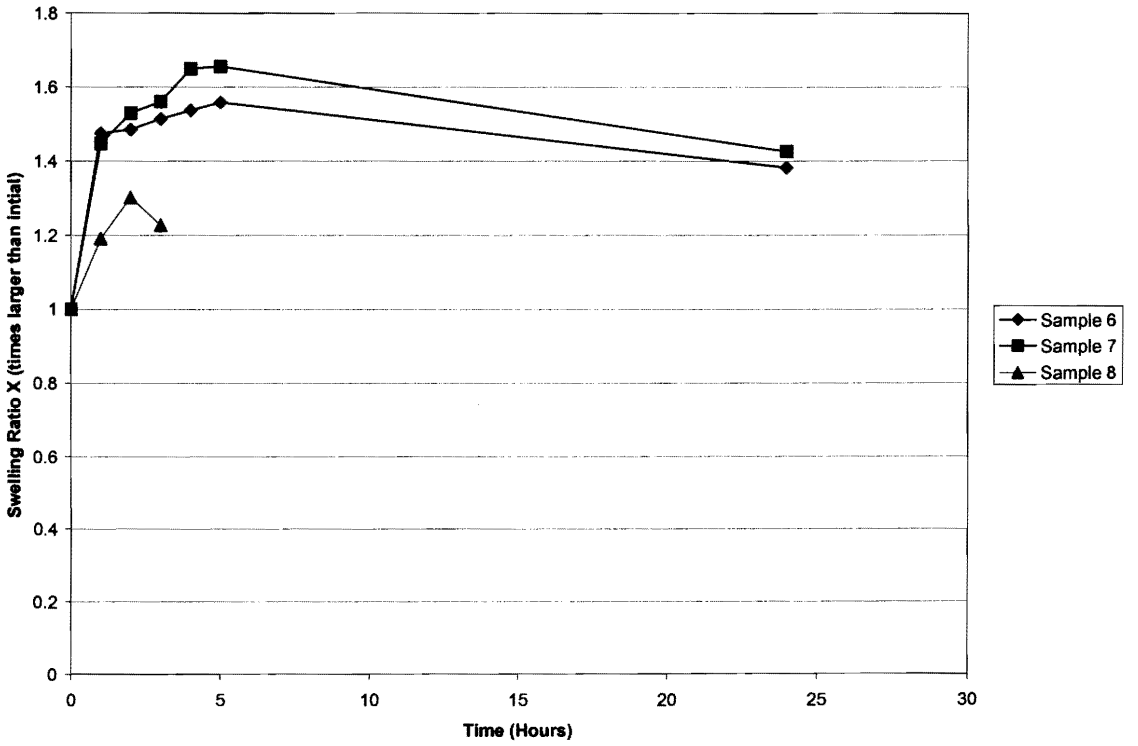

Figure 21. Swelling Ratio of PVA-H Versus Time in Simulated Body Fluid at 37°C.

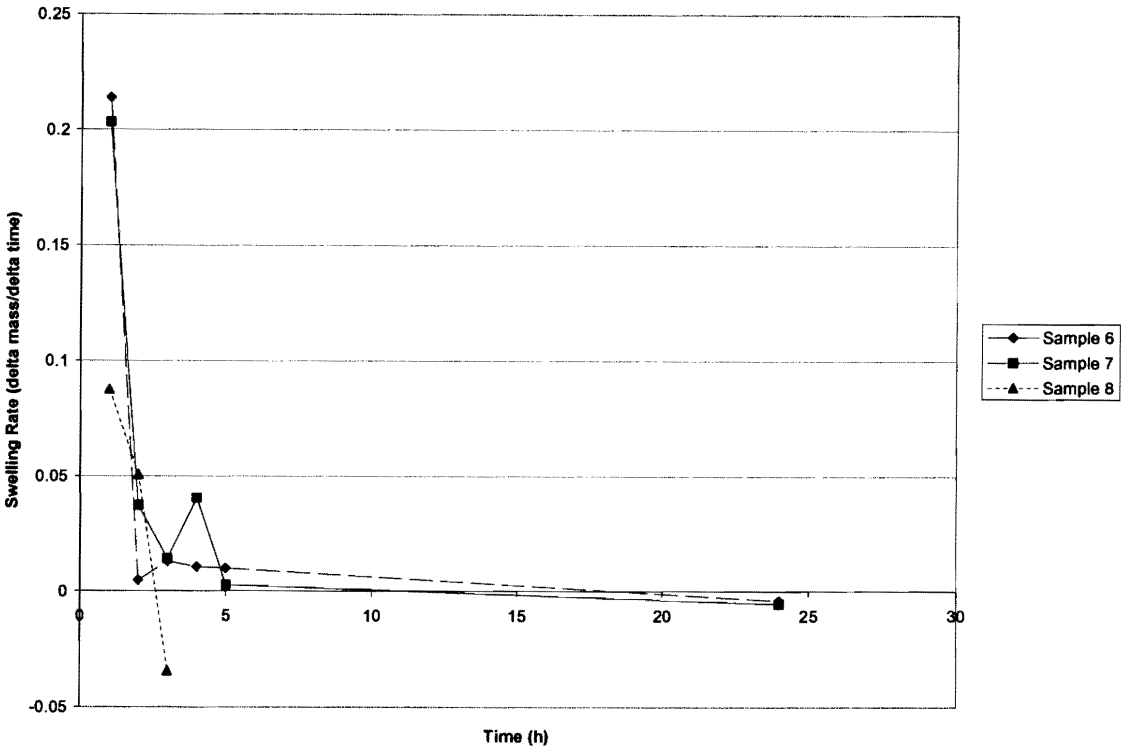

Figure 22. Swelling Rate of PVA-H Versus Time in Simulated Body Fluid at 37°C.

The final test used plasma as the swelling medium for the PVA-H. The PVA-H sample 9 was placed in plasma at 25°C that was obtained from the veterinary school. In order to prevent over-handling of the sample, an initial mass was taken and then a mass was taken every 24 hours afterwards. In 24 hours sample 9 had reached a swelling ratio of nearly 4X its initial size. The sample was measured again at 48 hours and the mass had decreased, but was still about 3.5X the initial size. Since measurements were not made every hour for the first few hours, the data correlating to swelling rate is not very useful. Clearly there was a significant amount of swelling that occurred in the first 24 hours. This trend may have continued after 24 hours, but by 48 hours the swelling had decreased. This test should really be rerun taking measurements couple of hours for the first 24 to 36 hours.

Hour	Mass (grams)	Swelling Ratio X	Swelling Ratio %	Swelling Rate
0	0.0434	1	100	0
24	0.1702	3.921658986	392.1658986	0.005283333
48	0.1543	3.555299539	355.5299539	-0.0006625

Table 10. PVA-H Test 3 in Plasma at 25°C—Sample 9.

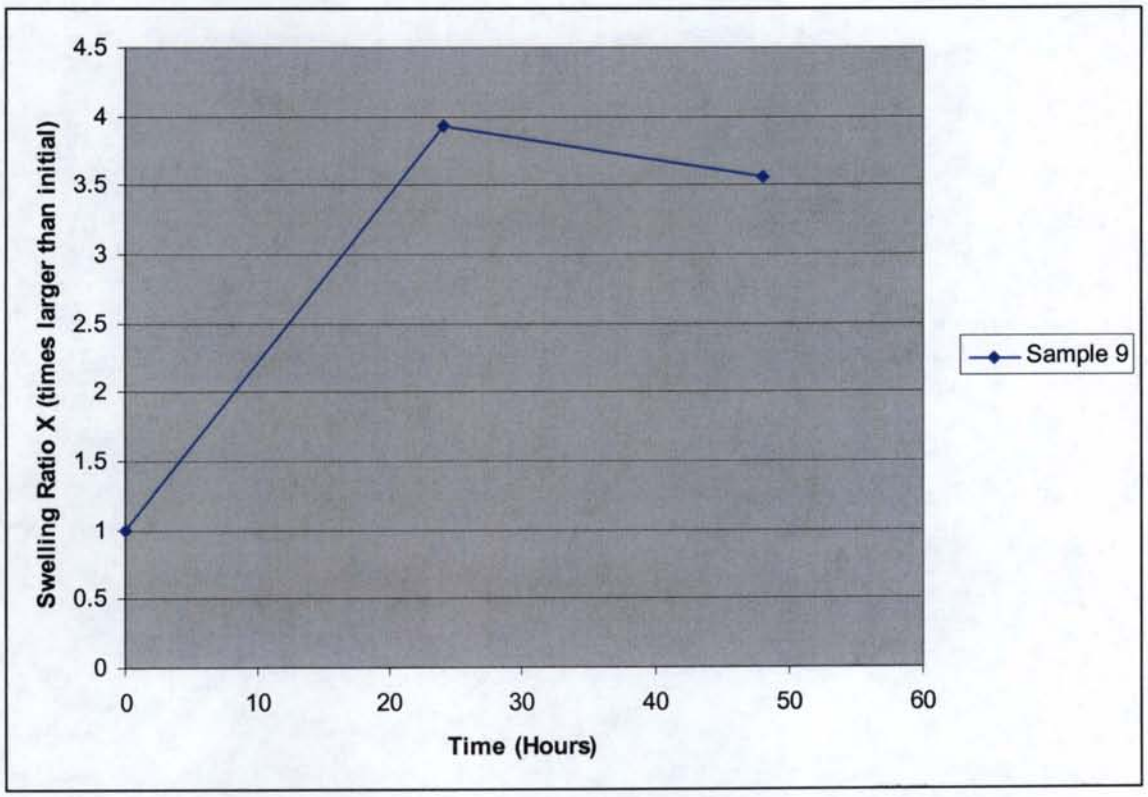

Figure 23. Swelling Ratio of PVA-H Versus Time in plasma at 25°C.

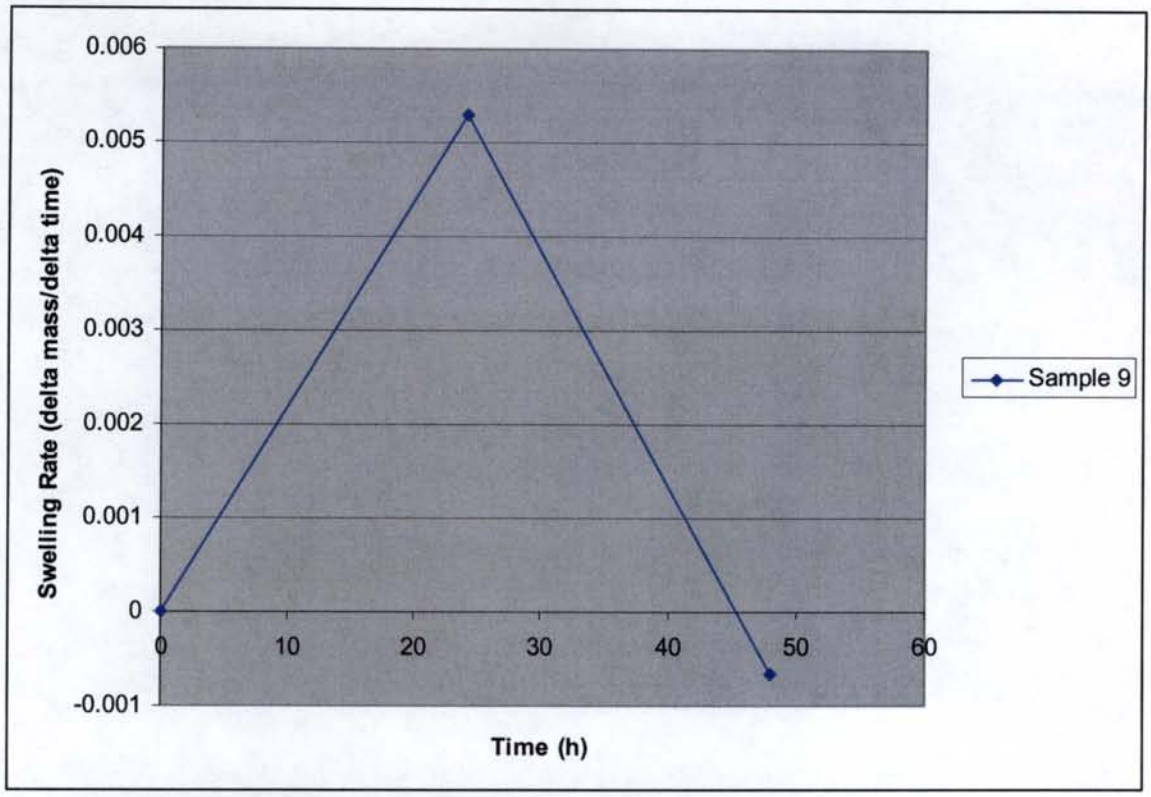

Figure 24. Swelling Rate of PVA-H Versus Time in Plasma at 25°C.

Note that volume measurements were not taken for a couple of reasons. First, our samples were very small and we did not have access to a graduated cylinder that would provide enough resolution to accurately measure the volume of the sample. Furthermore, an attempt at measuring the volume of the samples was made, but submerging the samples in an organic non-solvent increased the amount of handling and caused a more rapid degradation of the PVA-H which skewed the swelling ratio tests entirely. Thus, only mass measurements were used for the remainder of the tests and the test in which we attempted volume measurements was discarded.

Discussion

Testing of the PVA-H was used to measure how much water uptake would occur. In the first test, the water was at room temperature to give an approximation of the amount of swelling that would occur. Next, the temperature was raised to that of body

temperature, 37°C, which was hypothesized to increase the amount of swelling that occurred. The simulated body fluid utilized in the third test appeared to degrade the PVA-H at a quicker rate and caused the PVA-H to become more slippery and harder to handle. The eighth sample (the third sample of the third test) tore at the third hour during the mass measurement process. The breakdown of the PVA-H occurred more than was approximated from previous studies [6] and the durability proved to be less than predicted.

Cellular freeze/thaw PVA-H was selected for its good mechanical properties, excellent biocompatibility, high swelling rate, and high durability. The data from our tests proved that two of the four properties were not exhibited, these properties being high swelling rate and high durability. The biocompatibility was not tested directly, but many previous articles have proved this property to be more than adequate [6]. The biocompatibility would have been tested upon completion of the entire device by implantation *in vivo* in rabbits.

The swell ratio for the PVA-H was previously tested to be 7-8X its initial size, but our tests showed only a 1.5-2X its initial size in deionized water and simulated body fluid, and 4X its initial size in plasma. The increased temperature tests showed an increase in swelling in the deionized water tests. The simulated body fluid test was shown to have a swell rate similar to the test done in deionized water at 25°C. In previous articles outlining testing procedures [5], every hour the volume swelling ratio was measured, 5 mL of the deionized water was removed (for further testing of the degradation rate of the PVA-H) and 50 mL of fresh deionized water was added. The degradation rate of PVA-H exceeded the uptake of water after about the fifth or sixth

hour and caused a decrease in mass of the PVA-H. Consequently, a decrease in the PVA-H swell ratio was observed. Testing the PVA-H at body temperature expedited the degradation of PVA-H and gave worse results that the tests at room temperature. The simulated body fluid also caused an increased rate of PVA-H degradation. This is perhaps due to the amount of solutes in the fluid that could interact with and break the hydrogen bonds that formed physical crosslinks holding the PVA-H together. Surprisingly, the test of PVA-H in plasma gave the best results. The swell ratio was about 4X after a 24 hour period. The swelling did start to decrease sometime before 48 hours. The reason for increase swelling ratio in plasma as compared to the other tests is not known. This was a surprising result since the PVA-H exhibited limited swelling in the other testing media. Perhaps the plasma provides a more homeostatic environment for the PVA-H, thus reducing the amount of degradation and allowing the PVA-H to maintain its integrity. If PVA-H can maintain its structural integrity, it would then be able to uptake more water and thus have a higher swelling ratio.

The rate of swelling for each of the three tests varied. The first test (deionized water at 25°C) saw a high initial swelling rate, then a sharp decline in swelling rate the first 6 hours. Following the initial six hours, a more gradual decline in swelling rate occurred. The second test (deionized water at 37°C) showed a similar sharp decline in swelling rate as the first test, but to a negative swelling rate. After six hours, a gradual incline was observed. The third test (simulated body fluid at 37°C) followed the same initial sharp decline in swelling rate and then gradually declined after that. The final mass measurement was taken at 24th hour. At this time, the swell rate was observed to be negative. Between the two deionized water tests, the 25°C test sustained a positive swell

rate for the first 24 hours, while the 37°C displayed a negative swell rate after four hours. At 37°C, the simulated body fluid test saw a higher initial swell rate compared to the deionized water test. Also, the simulated body fluid test maintained a positive swell rate in the first 24 hours, whereas the deionized water test showed a negative swell rate at about hour four. In the 37°C deionized water test and the simulated body fluid test, the swell rates of the samples within each test were individually different compared to the 25°C deionized water test where the samples demonstrated similar swell rates. This difference could be due to the temperature change that had to occur to take mass measurements. The samples were taken from 37°C and exposed to room temperature while the measurements took place. Since the PVA-H tested in plasma was not measured for the first few hours, nothing can be concluded about the swelling rate other than it is most likely a positive rate for the first 24 hours and becomes a negative rate at some time between 24 and 48 hours. The reason sample 9 was not measured every hour is that we suspected that over-handling of the PVA-H was contributing to the high degradation rates.

The durability of the PVA-H was indirectly tested by examining it every time the mass was measured. In deionized water at 25°C, the PVA-H kept its integrity throughout the testing process. In the 37°C deionized water, the PVA-H began to show signs of degradation at approximately the fifth hour. The samples became stickier and began to fall apart slightly. In the simulated body fluid, the PVA-H began to degrade at the third hour. The samples appeared slippery when handled and one sample even degraded to such a great extent that mass measurements were no longer able to be taken. The durability of PVA-H in simulated body fluid had not been tested before, but PVA-H has

demonstrated good durability *in vivo*. Therefore, the possibility of the increased handling and transitions from a wet state to a dry state could be the cause of the decreased durability. The increased handling may have caused the samples to be stretched in ways that would not occur *in vivo*. With each mass measurement taken, the samples were blotted dry to ensure the mass measured was just that of the sample and not of excess water/fluid.

The mechanical properties of the PVA-H were not tested but could be measured by traditional methods given enough time. The pressure exerted by the PVA-H was also not measured due to lack of equipment and time. The proposed method for testing the pressure exerted is to take a polyethylene block and carve a hole in it the block in the shape of the occluder pressure plate. Next, the PVA-H would be heated and poured into the molded polyethylene and then allowed to set. Then a capacitive pressure sensor is placed on top of the PVA-H. A porous, mesh-like material that will allow water to reach the PVA-H but not allow the PVA-H to seep out of the mold is then used to cover the capacitive sensor and PVA-H. The entire contraption is submerged in water and the PVA-H swells against the pressure sensor and the pressure data is recorded.

Biodegrading copolymer of sebacic acid and 1,6-bis(carboxyphenoxy)hexane

Specifications

As discussed in detail within the section devoted to design of the portosystemic shunt occluding device, the actual mechanism for occlusion hinges upon a force generated through the swelling action of a hydrogel polymer. This swelling attempts to

move an occluder pressure plate, which in turn exerts the occluding force on the blood vessel. However, the rate at which the vessel is occluded, by this design, is controlled by biodegrading polymer cylinders, which constrain the motion of the occluder pressure plate and, thus, the swelling of the hydrogel. Consequently, whereas current shunt occluding devices such as rings of compressed casein rely on a slow and controlled swelling of a polymer, the device of this study attempts to utilize drastic and immediate, but constrained, swelling. Therefore, the occlusion rate is to be entirely a function of the rate of degradation of the biodegrading polymer. This shift of the rate limiting mechanism from the swelling polymer to biodegrading polymer is advantageous, given that ample research in biodegradable polymers has shown a great ability to finely control degradation rates.

Since, in the proposed design, occlusion rate is entirely a function of the biodegrading polymer pieces that prevent the occluder pressure plate mechanism from compressing the vessel, the choice of the degradable polymer is crucial in the materials selection process with many important considerations.

First, the overall mechanism of degradation must be considered. Since the percentage of vessel occlusion is entirely a function of the gradually decreasing diameter of the degrading polymer, only surface eroding polymers can be considered. Bulk-eroding polymers degrade not only from the surface but also throughout the polymer, resulting in an inability to control and utilize their unpredictably diminishing diameter to constrain the occluder pressure plate. Furthermore, bulk-eroding polymers experience a loss of mechanical stability as they degrade and will eventually reach a point at which they suddenly crumble, allowing the occluder pressure plate to compress abruptly and

drastically. On the other hand, surface-eroding polymers are capable of degrading so that mechanical stability remains largely intact as the overall diameter of the piece decreases nearly linearly in a highly predictable manner. As a result of surface erosion, the occluder pressure plate will gradually compress the vessel as the diameter of the polymer cylinders decreases. The rate at which these polymers degrade *in vivo* has been the subject of countless studies, and surface-eroding polymers have been fabricated that completely degrade in anywhere from days to years. For this intended application, it is desired to choose a surface eroding polymer that will degrade in a near-linear fashion in a three to four month period.

Next, biocompatibility concerns must be considered. Not only must the original polymer be safe for *in vivo* use, but all of its degradation products must also possess biocompatibility that allows for safe and effective metabolism and/or removal from the body. As mentioned above, biodegradable polymer research is extensive and ongoing, but such polymers have been approved and used in implants for many years. Because of their highly predictable and controllable degradation rates, they have been employed in a variety of drug delivery applications, most notably for cancer treatment, as well as in an assortment of load-bearing fracture fixation implants. Consequently, many compositions have been fabricated that have been proven safe within the body, and the final selection of polymer for this proposal is among many options.

Mechanical stability is also a minor concern. Since the polymer disks need only to withstand minor pressures from the occluder pressure plate/hydrogel, the selected polymer must remain mechanically intact as it degrades. However, the forces to be withstood are small, and the polymer is not load-bearing in the traditional sense.

Material

The selection of a biodegrading polymer for the proposed design must take into consideration all of the above concerns. Having already established that surface erosion is necessary, the search can be narrowed to biocompatible polymers with this mechanism. Since the vessel will be completely occluded before the polymer has entirely degraded (when the polymer diameter equals the thickness of the fully compressed shunt), in order to fulfill our goal time for total occlusion of three months, the selected polymer must have degradation rate slightly longer than three months. Consequently, polyanhydrides present the most likely solution to this material issue. Polyanhydrides have been extensively studied for their biocompatibility and highly controllable biodegradation. They have also been utilized in drug delivery systems [4]. Such polymers are known to have predictable surface degradation through hydrolysis within the *in vivo* aqueous environment.

To fulfill the desired specifications for the biodegradable polymer a surface-eroding, random copolymer of sebacic acid (SA) and 1,6-bis(carboxyphenoxy)hexane (CPH) was selected (see Figure 25). Previous studies have shown that PSA degrades very quickly (about 54 hours) while PCPH degrades much more slowly (around 1 year) [4]. Consequently, by varying the compositions of these two monomers, a polyanhydride copolymer could be fabricated with a degradation rate anywhere from around a month to a year [16]. The exact method by which the ratio of monomers for this application was determined is discussed in the synthesis section.

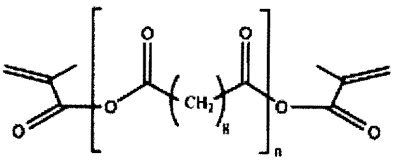

PSA

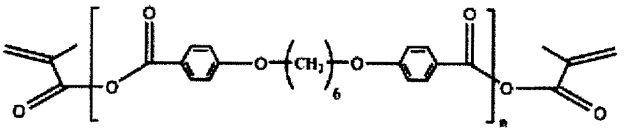

PCPH

Figure 25. This figure shows the chemical structure of poly(sebacic acid) and poly(1,6-bis (carboxyphenoxy)hexane. The proposed copolymer would be a random mixture of these repeat units.

Furthermore, although extensive proof has not been established, it seems that these copolymers possess adequate biocompatibility for this proposed design. Similar polymers (PSA-PCPpropane) have shown minimal inflammatory response when implanted subcutaneously in rats for 28 weeks and rabbits for 12 weeks. Loose vascularized tissue had grown into the rat implants at 28 weeks, with no evidence of fibrous encapsulation [9]. Such promising controlled degradation ability and biocompatibility has led to the development and marketing of PSA-poly 1,6-bis(carboxyphenoxy)propane Gliadel® implants for use in delivering the chemotherapeutic drug carmustine within the human brain. Clinical studies of these implants, as revealed on the Gliadel® package insert, have shown that carboxyphenoxy propane is eliminated by the kidneys, while sebacic acid is metabolized by the liver and expired as carbon dioxide in animals. As a result, it is a reasonable assumption that the degradation products of the proposed sebacic acid and carboxyphenoxy hexane copolymer can be metabolized and excreted safely as well.

The selection of PSA-PCPH to serve as the occlusion rate-limiting, biodegradable polymer attempts to meet all of the desired specifications for this application in a safe, well-understood manner. Literature supports that such a copolymer is reasonably safe and biocompatible for use in implants and degrades in a highly controllable, highly predictable surface-eroding manner that will ensure mechanical stability throughout degradation.

Method of Synthesis

The fabrication of a copolymer of sebacic acid and carboxyphenoxy hexane took place in two major steps. First, the monomers must be formed and methacrylated through a series of detailed syntheses steps. Then, the methacrylated monomers are polymerized together to form a random copolymer.

Synthesis of Methacrylated Sebacic Anhydride (MSA) monomer

The protocol selected for synthesizing this monomer has been published in literature and provided a fairly detailed account of synthesis [10]. First, 10 grams of sebacic acid was refluxed with 2.5 M equivalents (~19 grams) of methacrylic anhydride in a dry argon gas environment until the sebacic acid was fully dissolved. The established protocol cited a 1 hour reflux time; however, the sebacic acid was only fully dissolved after many hours of refluxing in a 200 degree Celsius sand bath. The solution was allowed to cool and then vacuum distilled to remove excess methacrylic anhydride. The remaining sebacic anhydride was then purified by dissolving in methylene chloride and precipitation in petroleum ether. The resulting MSA precipitate was then filtered and

dried. The theoretical yield was calculated to be 25.38 g. The actual yield was 7.0241 g. Thus, the percent yield was 26.675%. The low yield was most likely a result of inexperienced chemists, the difficulty encountered in getting the reaction to reflux, the reaction not going to completion, and the possible hydrolysis of the product after purification and crystallization since it was not stored under argon at subambient temperatures [10].

Both proton nuclear magnetic resonance (^{1}H-NMR) and Fourier transform infrared spectroscopy (FTIR) were utilized to confirm the product identity. ^{1}H-NMR (Figure 26) imaging compared extremely well with the expected results for MSA found through ChemNMR H-1 estimation. Two small peaks at 5.8 and 6.2 ppm reveal the presence of the hydrogen end groups of the methacryl functional units. Also, the peak groups near 1.3, 1.6, 2.0, and 2.4 ppm represent the eight CH_2 units in the middle portion of the sebacic molecule. An integration of the peaks at 2.4 revealed a value of 14.10, whereas integrations of the methacryl peaks at 5.8 and 6.2 gave values of 1.51 and 2.00 respectively. By determining the ratio of sebacic portions to methacryl end groups (with 1 sebacic group per 2 methacryl end groups for pure monomers), the degree of polymerization of the monomers can be estimated. The nearly (3 sebacic):(2 methacryl) peak ratio reveals that the resulting product was not entirely pure monomer, but rather on average 3 unit oligomers. However, for the purposes of synthesizing a random copolymer, these oligomers are likely sufficient. Likewise, FTIR (figure 27) provided strong evidence that the reflux had yielded the expected MSA monomer/oligomers. Principally, the 2 absorbance peaks near 1700-1800 wavenumber (cm^{-1}) reveal the carbonyl stretches that are attributable to anhydrides. Also, the peaks near 3000 cm^{-1}

reveal the alkene stretches. Similarly, C-O stretches are also confirmed by the series of peaks near 1100 cm^{-1}.

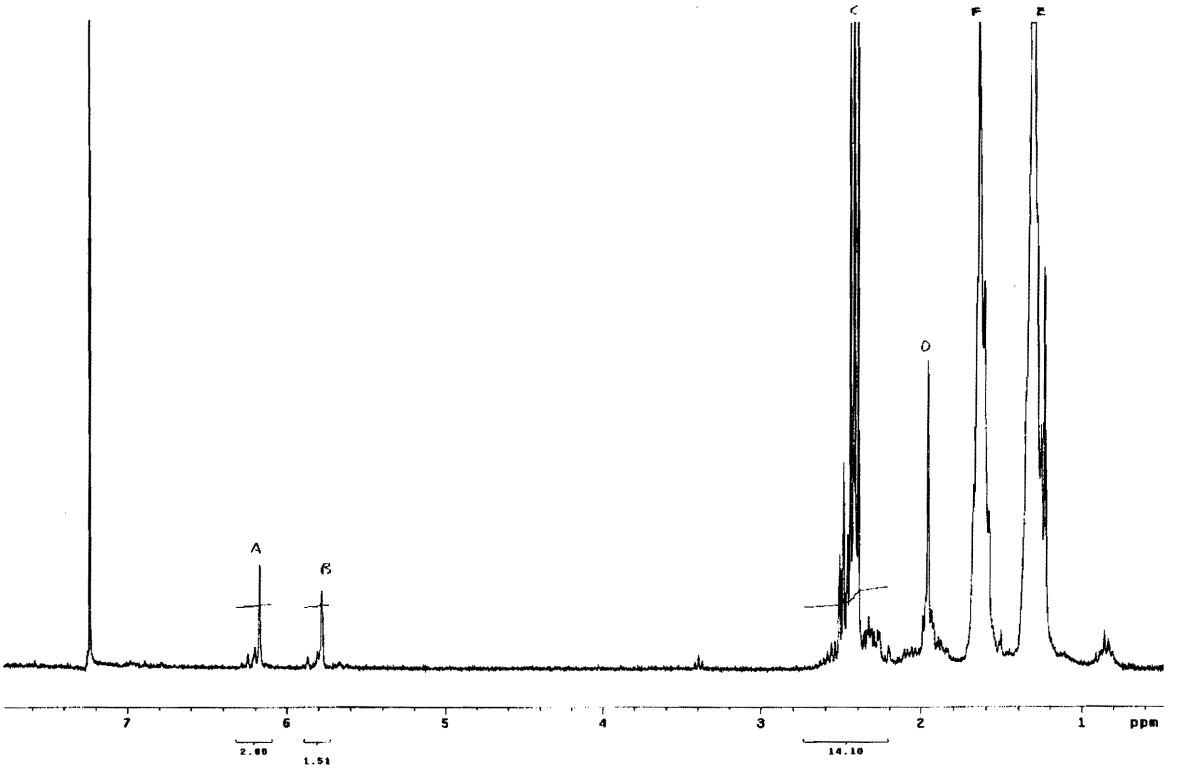

Figure 26. NMR-H1 of methacyrlated sebacic anhydride (above) with ChemNMR Estimation (below)

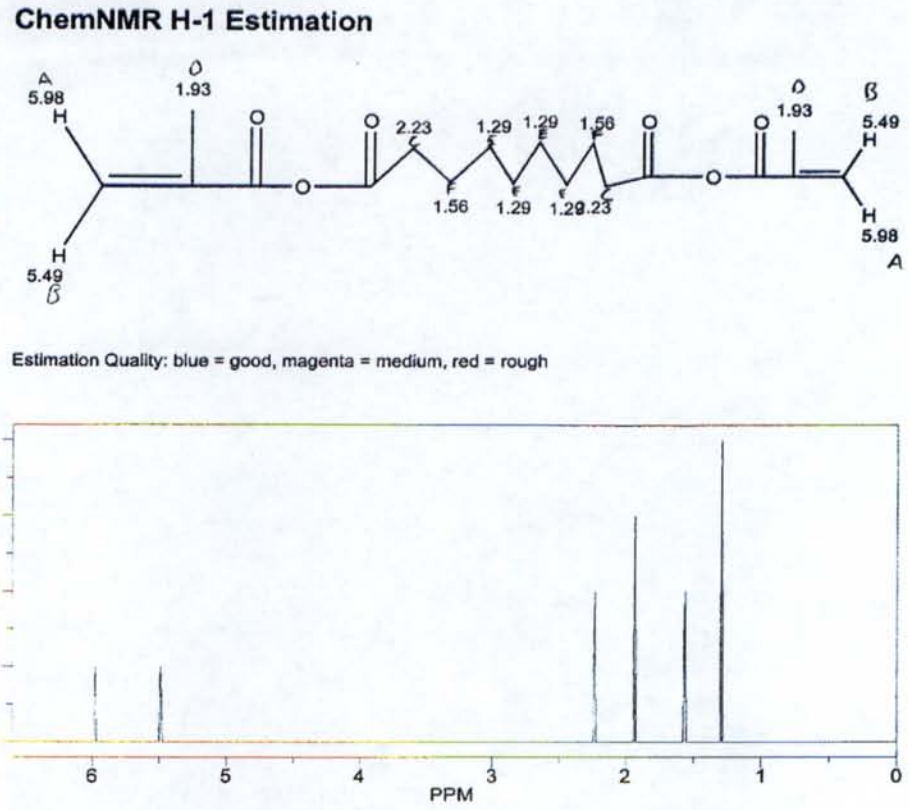

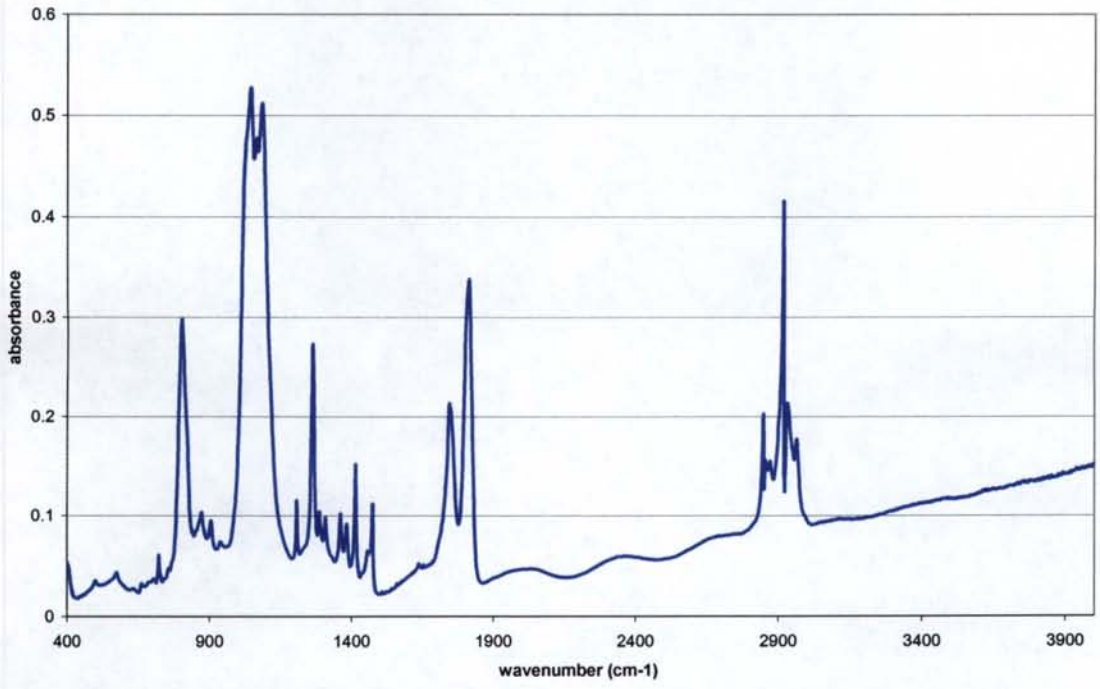

Figure 27. IR spectrum for methacrylated sebacic anhydride product

Synthesis of Methacrylated 1,6-bis(carboxyphenoxy)hexane monomer (MCPH)

The synthesis protocol for the fabrication of MCPH was followed from a 1966 paper published in *Macromolecular Syntheses* [3]. This literature source provides the protocol for synthesizing methacrylated 1,6-bis(carboxyphenoxy)propane; however, the similarities between these molecules allow the substitution of the hexane form of the molecule without any change to the protocol.

First, in a three necked flask, 13.8 grams of p-hydroxybenzoic acid was mixed with 8 grams of sodium hydroxide in 40 mL of water. Then, 10.2 grams of 1,6-dibromohexane was added from a dropping funnel over the course of an hour while a stirring bar assisted in the mixing process. The mixture was refluxed at 100 degrees Celsius. After the addition of 1,6-dibromohexane was completed, the solution was refluxed for an additional 3.5 hours. Then, 2 grams of solid sodium hydroxide was added to the mixture. This mixture was refluxed for an additional 2 hours and at this point left overnight. The following day, the precipitate of the disodium salt was isolated through filtration and washing with 20 mL of methanol. This wet precipitation was then dissolved in 0.10 L of distilled water. The solution was then warmed to 60-70 degrees Celsius and acidified with 6 N sulfuric acid. While still warm, the dibasic acid was isolated by filtration and dried in a vacuum oven at 80 degrees Celsius. The theoretical yield should be 7.9 grams (or 50 percent), and the neutralization equivalent is 157 (calc. 158). An NMR on dibasic acid was used to verify identity of this intermediate product (Figure 28). Aliphatic groups are represented at 1.75 and 1.4 ppm. Most importantly, the broad peak between wavenumber three and four denotes the hydroxyl groups that are

within the carboxylic functional units. Furthermore, pairs of peaks at 6.8, 7.0, 7.7., and 7.9 ppm represent the benzene rings within the acid.

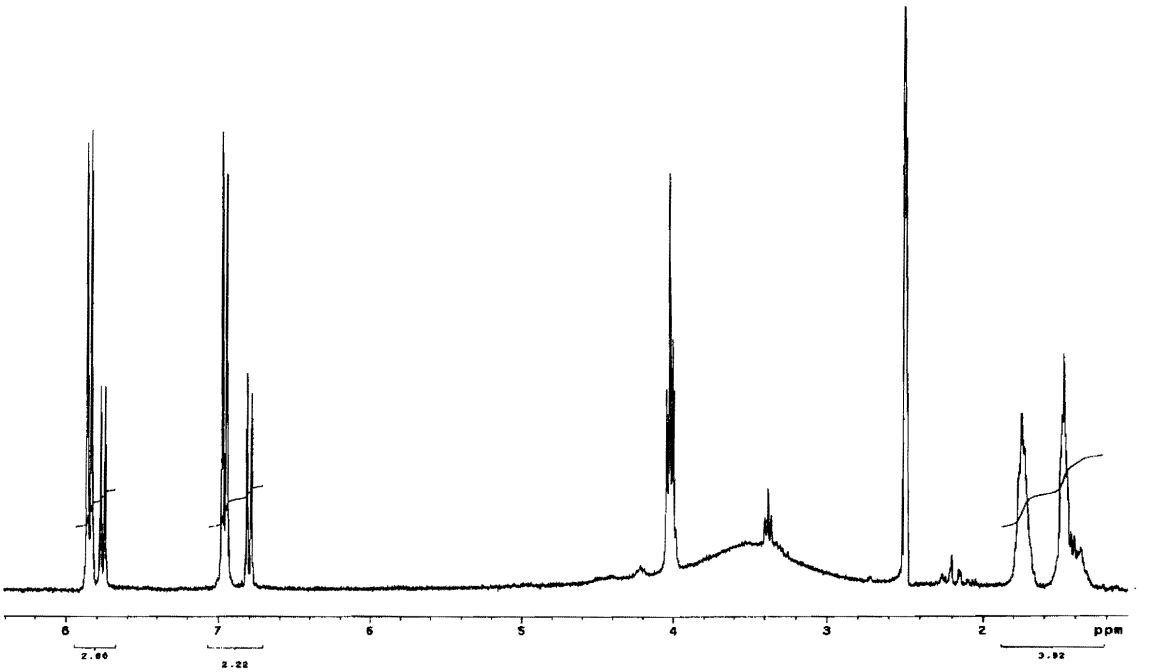

Figure 28. NMR-H1 for the dibasic acid intermediate product within the MCPH synthesis

Next, in a three necked flask fitted with a stirrer, a condenser, and a gas inlet tube for dry argon are placed 1.6 grams of 1,6-bis(p-carboxyphenoxy) hexane (the product from the above reaction) and 20 mL of acetic anhydride. The mixture was refluxed for about 7 hours until a majority of the 1,6-bis(p-carboxyphenoxy)hexane was dissolved. The solution was then allowed to cool. Next, the solution was distilled under vacuum at a vapor temperature of 27 degrees Celsius to concentrate the solution by a factor of 5. The remaining solution was kept and allowed to crystallize. FTIR was run to ensure the product identity of this anhydride of 1,6-bis(carboxyphenoxy)hexane (Figure 29). The noteworthy peaks in this IR spectrum are the anhydrous peaks around 1800 cm^{-1} and the disappearance of the carboxylic peak that would have existed above 3400 cm^{-1} if the reaction had been unsuccessful.

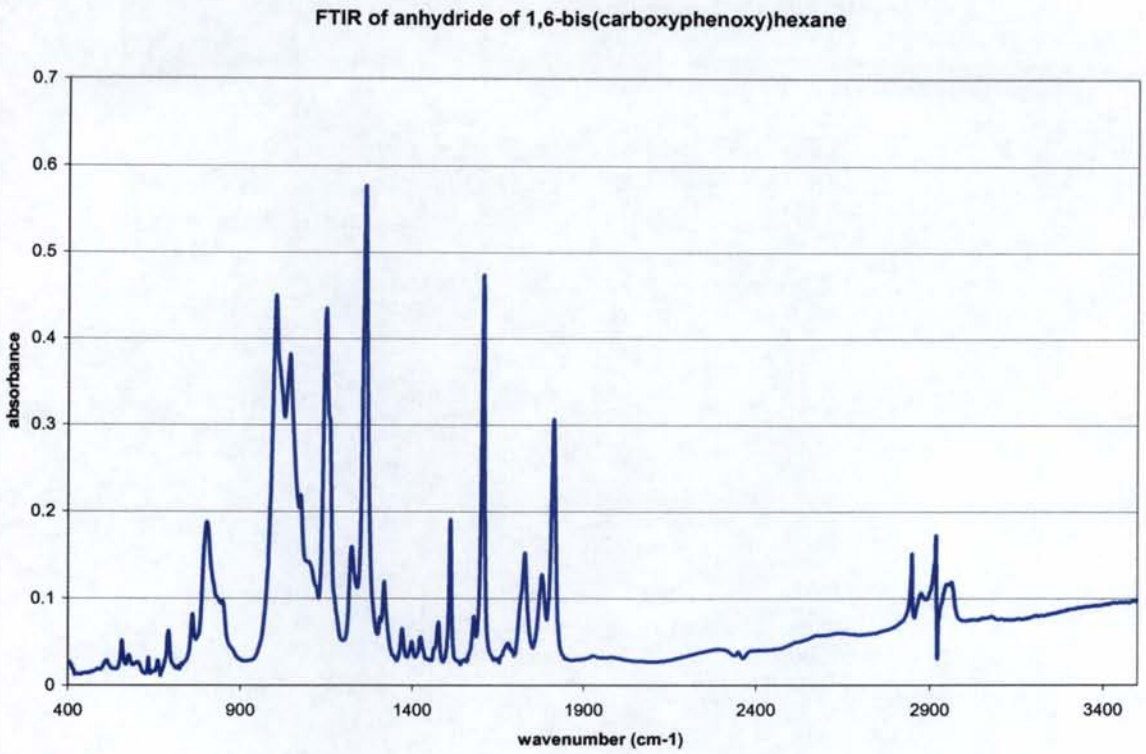

Figure 29. FTIR analysis of the anhydride of 1,6-bis(carboxyphenoxy)hexane

However, it was desired to then methacrylate these 1,6-bis(p-carboxyphenoxy)hexane monomers (as was done to the MSA) before the copolymerization procedure. Consequently, the crystals were dissolved and refluxed in excess methacrylic anhydride. The reaction was carried to completion and then allowed to cool. Since amounts used in the initial reactions were relatively small, there were not many crystals to dissolve into the solution. Thus after the reflux, the product was not vacuum distilled for fear that there would not be enough product left after distillation to crystallize. Instead, the product was allowed to crystallize without undergoing distillation. After the crystals formed, they were dissolved in methylene chloride and precipitated in petroleum ether. The resulting crystals were very impure and their molecular structure was not able to be confirmed due to time limitations. The final

crystals took too long to dry and we were unable to continue the copolymerization. Had more starting reagents been used from the beginning, there most likely would have been enough methacrylated CPH to allow vacuum distillation and thus enable a greater amount of pure crystals to be used in copolymerization. Additionally, a fair amount of each monomer is needed for melt condensation of a polymer, and even if the MCPH had been pure, there may not have been enough to carry out a polymerization reaction.

Copolymerization

Having both monomers methacrylated, the final step to synthesis of the desired biodegrading polymer is copolymerization with the proper monomer ratio. As discussed previously, the goal of this synthesis is to produce a copolymer of sebacic acid and 1,6-bis(carboxyphenoxy)hexane that will fully degrade over a period of three months. The first step for making a determination of the required monomer ratio is to determine the degradation rates for varying compositions of this copolymer. Data has been published for the percent mass loss of varying poly(MSA:MCPH) as a function of degradation time in phosphate buffered saline solution [10]. The tested ratios consist of 1:0, 50:50, 40:60, 25:75, and 0:1 MSA to MCPH respectively. If these curves (Figure 30) are extrapolated to 100% mass loss the 50:50 copolymer degrades in ~10 days, the 40:60 copolymer in ~79 days, and the 25:75 copolymer in ~195 days. This published data was used in this design project for the purpose of determining the composition that could be expected to yield a copolymer that would fully degrade in a 3 month period. In order to accomplish this goal, the time to 100% mass loss was graphed as a function of the amount of MSA in the molar ratio (Figure 31). It was noted that the region from 0:1 (MSA:MCPH) to 40:60

(MSA:MCPH) was nearly linear, and a linear regression trendline for this portion was determined. The trendline yielded the equation [**y** = (-172.31)**x** + 8870.3], where y is the time to total degradation (in hours) and x is the amount of MSA in the molar ratio. Since the desire is to obtain total occlusion at three months, which should occur before the polymer is fully degraded, a target time of 3.5 months (~2500 hours) until complete mass loss was set. By using the trend established above, it was determined that a copolymer with a 37:63 molar ratio of MSA to MCPH could be expected to yield the desired specification of just over 3 months until total degradation.

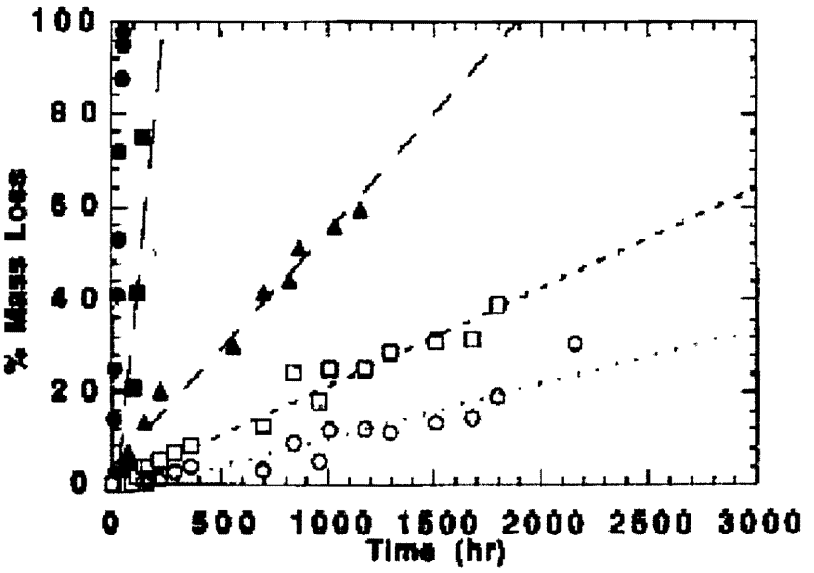

Figure 30. Cumulative percent mass loss as a function of degradation time for crosslinked polymers of varying composition: poly(MSA) (solid circle), 50:50 poly(MSA:MCPH) (solid square), 40:60 poly(MSA:MCPH) (solid triangle), 25:75 poly(MSA:MCPH) (hollow square), and poly(MCPH) (hollow circle).

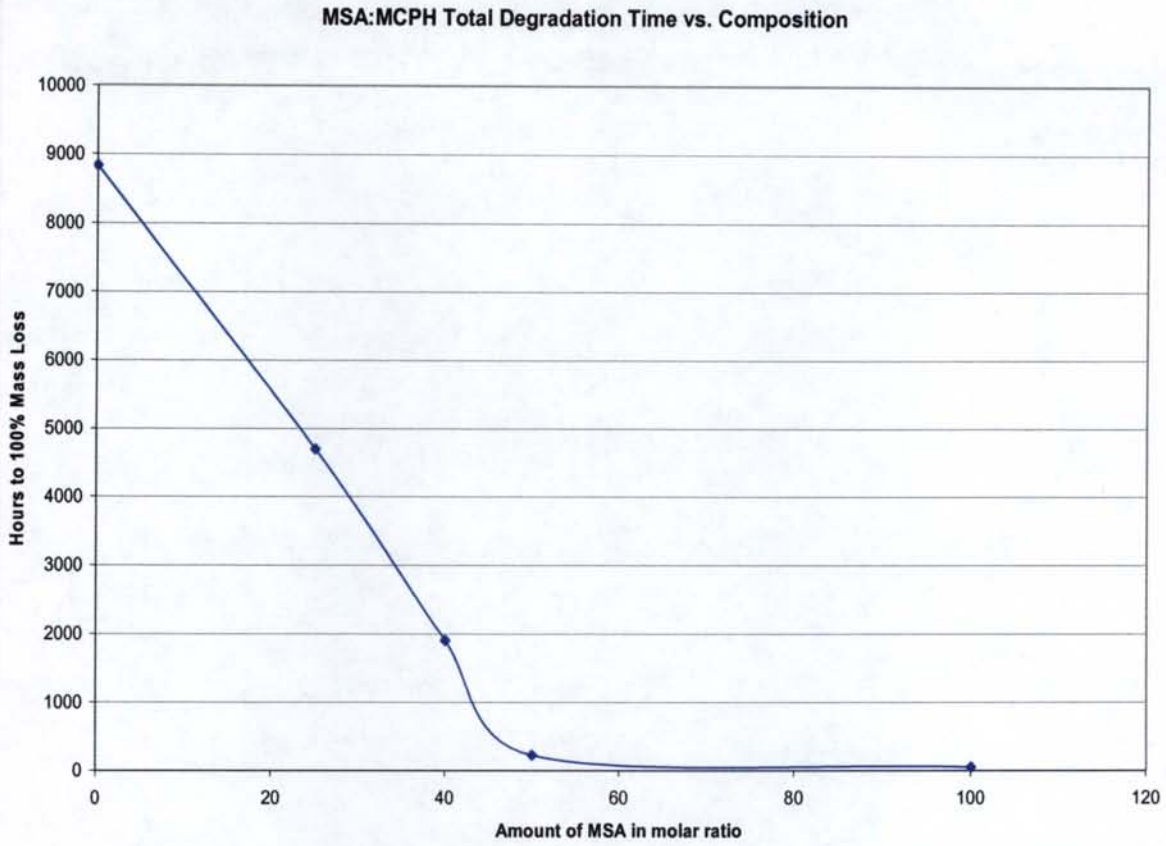

Figure 31. Time to total degradation as a function of the amount of MSA in the molar ratio of the copolymer. Actual data comes from Muggli et al. [10].

Unfortunately, the synthesis process for methacrylating and preparing the MSA and MCPH monomers was much more difficult and time consuming than expected. Furthermore, the MCPH yield was extremely low for this synthesis procedure. Consequently, a lack of time and monomer yield prohibited this copolymerization and the testing to follow from occurring.

Blue light in the and a corresponding photoinitiators camphorquinone and ethyl-4-N,N-dimethyl aminobenzoate were used to copolymerize this polymer in the literature [16]. Ultraviolet light has also been used with the photoinitiator 2,2-dimethoxy-2-phenyl-acetophenone [10]. Blue light is the preferred method of copolymerization since

it has better "penetration of the light to larger depths than UV systems due to the tendency of camphorquninone to quickly photobleach" [16].

The copolymerization would have been accomplished by melt condensation under high vacuum at 180°C as described in Piszczek et al [12]. The apparatus would be connected to a distillation column in order to distill off the methacrylic anhydride that forms as a byproduct of this polymerization. The reaction requires approximately 90 minutes and the product should be stored under argon in a dessicator under vacuum to prevent hydrolysis. Due to very small yields as a result of many steps in the synthesis and inadequate starting amounts of reagents, and failure to attain purified MCPH the copolymerization was not able to be attempted.

Testing and Results

As aforementioned, the amount of time required to perform the sophisticated synthesis procedure was significantly underestimated and no time remained to fabricate the final copolymer and sufficiently test its characteristics. However, if time permitted a variety of tests had been planned to determine how well poly(37MSA:63MCPH) met the desired mechanical and degradation specifications.

First, several mechanical characteristics would have been ascertained. Differential scanning calorimetry would have been performed to determine the glass transition temperature. Also, compression tests would be performed to determine the elastic modulus, tensile strength, deformation characteristics, etc.

Most importantly, several experiments must be executed in order to document and understand the degradation characteristics. The testing fluids would have consisted of

separate degradations in deionized water, simulated body fluids, and blood plasma. The measurables of such experiments are mass loss as a function of time, diameter as a function of time, and a qualitative confirmation of surface degradation rather than bulk-erosion. Also, it would be noteworthy to perform periodic compression testing throughout the degradation process to ensure that the copolymer remains sufficiently mechanically stable as it degrades. If needed, these tests could be done more quickly using a time-temperature superposition experiment.

Discussion

Despite the lack of tangible results from the massive efforts invested in attempting to synthesize the poly(MSA:MCPH), much was learned through way of experience throughout the process. Much profitable time was spent pouring through published literature, which greatly enhanced the amount of previous knowledge the team members possessed in the realm of polymers and synthesis chemistry. The synthesis steps themselves taught a great deal about the many methods used for polymerization, and the laboratory skills of everyone involved have increased immeasurably. Furthermore, utilization of proton NMR and FTIR as a method of confirming and characterizing both the intermediate and final products yielded a much greater awareness of how to employ these powerful tools to gain a better understanding of synthesis.

Time permitting, the design team was confident that this process could have yielded a copolymer with extremely promising characteristics that would have fulfilled the specifications for mechanical stability and degradation rates established as part of the overall design. All literature and preliminary results strongly suggest that with enough

time and resources, the synthesis undertaking would have been fairly successful. Furthermore, NMR and FTIR characterizations, as discussed in the synthesis section above, prove that the synthesis steps undertaken were successful and resulted in the expected intermediates. However, with that said, the process undertaken revealed a few flaws as well, which could be amended in future work. Mainly, the false assumption that there would be enough time to run through the entire synthesis procedure more than once resulted in the decision to run the first trial with a relatively small amount of reagents. However, as time to complete the fabrication of the polymer and test its degradation rates became shorter, it became apparent that the first synthesis attempt should have been done at full scale. Consequently, if the synthesis was successful in one attempt, enough copolymer would have been produced to perform all of the necessary characterizations, degradation testing, and device fabrication. On the other hand, when the amount of time that could be invested in synthesis was exhausted, the results from each step had been promising and supported the idea that such a synthesis procedure could be fully successful.

Overall Project Conclusions and Limitations

The novel design of a portosystemic shunt occluder was not fully completed; however, given some of the major problems that surfaced during the fabrication and testing of certain aspects of the design, the design is likely to have limited success as it stands. Modifications could definitely be made to the design to improve its effectiveness and perhaps have more success. The design concept is sound, but when considering the size of the device, the design is impractical. Likewise, the concepts behind the material

selections are reasonable and accurate based on the literature, but once in the experimental phase the PVA-H in particular proved to be inadequate. The other material selections, however, appeared as though they would have been successful. Definitely high-density polyethylene would have provided more than enough mechanical strength needed for exerting such minute forces. Additionally, the biodegradable polymer selection seemed promising. While the polymer's degradation rate and properties were not able to be tested, the synthesis was successful up to the methacrylation of CPH which only failed due to extremely small yields. There is no guarantee that if the copolymer had been synthesized that it would have functioned as well as stated in the literature, but theoretically the degradation rate should have been sufficient. While the percent yield of MSA was calculated, the percent yield of the MCPH was not able to be calculated as there was not enough pure product obtained to be measured. In retrospect, the percent yield should have been calculated at each step in the synthesis, but, due to a lack of experience, the intention was to calculate a percent yield of only the MCPH, MSA, and the random copolymer had it been synthesized. While the biocompatibility of the chosen materials was not directly tested, there is extensive, well-documented literature confirming their biocompatible properties.

This project was indeed quite ambitious for a one-year senior design project. Although not much was accomplished when considering a finished, functional device, much has been learned in the process that will aid in advancing future designs and hopefully eventually develop a solution to the problem of extrahepatic portosystemic shunts. After considering all of the problems encountered during the design process, two emerged as the most significant.

First, the inability to obtain an appropriate swelling ratio from the physically crosslinked PVA-H would have rendered the device ineffective. As discussed previously, a swelling ratio of at least 7-8X the initial volume of PVA-H is needed to achieve full occlusion, but the PVA-H was only able to achieve a swelling ratio of 4X and then only in the plasma media. Granted, the plasma media is the most important test, but there was not enough time to rerun the experiment to see if the results were repeatable. The physically crosslinked PVA-H degraded much too quickly in the other experiments to have been used in a permanent device. The degradation most likely occurred so quickly because the physically crosslinked PVA-H relies on hydrogen bonding for its crystalline structure, and hydrogen bonds will be broken in an aqueous environment given enough time. Perhaps if the PVA-H had been chemically crosslinked, it is possible that its durability and swelling ratio properties would have been improved thus making it suitable as the hydrogel for the current device.

The second, and probably the hardest, limitation to overcome is the difficulty in machining such a small device with so many mechanical parts. Such a device is unrealistic and is not cost effective. The current design has overall dimensions of 16.5 mm x 13.5 mm x 3mm. Included in this design are four moving parts. Trying to fabricate four moving parts in a device of this scale, which must be done mostly by hand, is extremely difficult and tedious. Not to mention that being able to set up a manufacturing process for such a device, had it been successful in occluding a shunt, would most likely be impossible. Furthermore, a device that requires the surgeon to adjust too many moving parts is cumbersome and unfavorable. A device that has a design considered unfavorable by surgeons will not survive in the market.

The above limitations are severe barriers to obtaining a successful and marketable device. The information and research obtained from this novel device is invaluable in carving the future of extrahepatic portosystemic shunt occluders, but much future work is needed.

Future Work

Given more time and resources, the desired 37MSA:63MCPH composition biodegradable copolymer needs to be synthesized to completion. After synthesis, it should be tested for its degradation rate and properties and resynthesized with modified composition of MSA:MCPH until the desired degradation rates and mechanical properties are obtained. Next, the PVA-H would be chemically crosslinked and retested to see if its swelling ratio attains the needed 7-8X. If PVA-H still does not reach the desired swelling ratio, then selection of a new hydrogel should be investigated. Furthermore, assuming that chemically crosslinking PVA-H provides the needed swelling ratio and that the biodegrading copolymer of MSA:MCPH has the appropriate degradation rate and properties, the entire device should be tested *in vitro* to verify that the device will function in the absence of a vein. Then the device should be tested again *in vitro*, but this time with an experimental setup that mimics the *in vivo* environment as closely as possible, perhaps using tubing of some sort to mimic the vein and the venous pressure. Once both of these tests have been completed, then the device should be tested *in vivo* in rabbits. If the device is successful in rabbits, then it can be prototyped and tested in dogs. Before testing in vivo, appropriate sterilization techniques must be

determined in order to safely sterilize the device without damaging its integrity, materials, or functionality.

Another avenue of future work involves reducing the number and complexity of the moving parts in the design while maintaining the general concept of the design. If the design could be modified, or if an entirely new design could be developed, using the same concepts, and thus the same or similar materials to those used in this project, so that the device could be more easily machined, then the chances of success of such a device would be greatly increased. Much of the ground work for developing a second generation novel device has already been completed, assuming that the second generation device maintains the conceptual design of the first generation. Taking the information obtained from the current first-generation design, and investing enough time and thought to create a second-generation design would no doubt be rewarding and beneficial in solving this problem.

In addition to the above work, the design alternatives would have been studied. Most notably, controlling the swell rate of the current device via the sputtering of the current device through a mask would have been tested. This idea would have been rather simple to complete and test. After testing, the effectiveness of masking the casein could be compared to the novel design. Masking the casein in the current constrictor could very likely have been more successful at achieving the needed occlusion rates. If the idea had worked, it would have undoubtedly been much more simple and easier to fabricate, manufacture, and use than the current design.

Acknowledgements

The authors would like to extend great thanks to the many people that assisted them throughout this entire project. Dr. Roberto Benson, their advisor, for his encouragement, support, and guidance as he served as their mentor. His immediate receptiveness of them as a part of his lab group aided them throughout the entire process. Libby Barker, for her constant support in finding the proper materials and connecting them with the proper people each step of the way was an invaluable part of this project. Deepali Kumar, for her assistance with the synthesis of their polymers. The many hours she spent allowing the authors into her lab and keeping them on track throughout the synthesis cannot be given enough thanks. Riyam Kafri, for her help with the distillation of their polymers. Douglas E. Fielden for his feedback and ideas in developing a machinable device and his diligent work in machining their extremely difficult and tedious device. Chris Stephens, for his consultations in matters of materials science and engineering. Dr. Karen Tobias from the veterinary school for answering all of their many questions. Dr. DJ Krahwinkel, from the veterinary school for donating the authors the plasma needed for some of the testing. Dr. Masood Parang and Dr. William Hamel, for their monetary contribution, which made the project possible. Dr. Mark Luprecht, for his support as their honors program advisor for this project.

Without the contribution of each and every person, this project would not have been the successful learning experience that it turned out to be.

References

1. Adin, Chirstopher A. et al. Effect of Petrolatum Coating on the Rate of Occlusion of Ameriod Constrictors in the Peritoneal Cavity. *Veterinary Surgery*. **33**: 11-16. 2004.
2. Atta, Ayman M and Karl-Friedrich Arndt. Characterization of strong polyelectrolyte hydrogels based on poly(vinyl alcohol). *Polym Int*. **54**: 448-455. 2005.
3. Conix A., Poly[1,3-bis(p-carboxyphenoxy) propane anhydride]. *Macromol Synth*. **2**: 95-96. 1966.
4. Gunatillake, Pathiraja A. and Raju Adhikari. Biodegradable Synthetic Polymers for Tissue Engineering. *Cells and Materials*. **5**: 1-16. 2003.
5. Hassan, Christie M., and Nikolaos A. Peppas. Cellular PVA Hydrogels Produced by Freeze/Thawing. *J of Applied Polymer Sciences*. **76**: 2075-2079. 2000.
6. Kobayashi, Masanori, Jyunya Togushida, and Masanori Oka. Development of an artificial meniscus using polyvinyl alcohol-hydrogel for early return to, and continuance of, athletic life in sportsperson with severe meniscus injury. I: mechanical evaluation. *The Knee*. **10**: 1, 47-51.
7. Kyles, Andrew E., Elizabeth M. Hardie, Margo Mehl, and Clare R. Gregory. Evaluation of ameroid ring constrictor for the management of single extrahepatic portosystemic shunts in cats: 23 cases (1996-2001). *JAVMA*. **220**: 9, 1341-1347. 2002.

8. Lange, P.E. et al. A new device for slow progressive narrowing of vessels. *Basic Res Cardiol.* **80**: 430-435. 1985.

9. Laurencin, CT, HM Peirrie –Jacques, and R Langer. Toxicology and biocompatibility considerations in the evaluation of polymeric materials for biomedical applications. *Clin Lab Med.* **10**: 549-570. 1990.

10. Muggli, Dina Svaldi, Amy K. Burkoth, and Kristi S. Anseth. Crosslinked polyanhydrides for use in orthopedic applications: Degradation behavior and mechanics. *J of Biomedical Materials Research.* **46**: 271-278. 1999.

11. Paradossi, Gaio, Francesca Cavalieri, and Ester Chiessi. Poly(vinyl alcohol) as versatile biomaterial for potential biomedical applications. *J of Materials Science: Materials in Medicine.* **14**: 687-691. 2003.

12. Piszczek, Robert, Brianne Dziadul, Elizabeth Shen, and Balaji Narasimhan. Differential scanning calorimetry studies of crystalline morphology in bioerodible polyanhydrides for drug delivery. *Electronic Bulletin of Undergraduate Research.* http://rutgersscholar.rutgers.edu/volume02/narapisz/narapisz.htm. 2000.

13. Ratner, Buddy, Allan Hoffman, Frederick Schoen, and Jack Lemons, Eds. Biomaterials Science: An Introduction to Materials in Medicine. Elsevier Academic Press. San Diego, CA 1996.

14. Sereda, Colin W. and Christopher A. Adin. Methods of Gradual Vascular Occlusion and Their Application in Treatment of Congenital Portosystemic Shunts in Dogs: A Review. *Veterinary Surgery.* **34**: 83-91. 2005.

15. Tas, AC. Synthesis of biomimetic Ca-hydroxyapatite powders at 37oC in synthetic body fluids. *Biomaterials* **21**: 1429-1438. 2000.

16. Temenoff, Johnna S. and Antonios G. Mikos. Injectable biodegradable materials for orthopedic tissue engineering. *Biomaterials*. **21**: 2405-2412. 2000.

17. Tobias, Karen. Unviversity of Tennessee College of Veterinary Medicine. Portosystemic Shunts. http://www.vet.utk.edu/clinical/sacs/shunt/. Accessed 29 April 2005. © 2005.

18. Vogel, Brandon M., Surya K. Mallapragada, and Balaji Narasimhan. Rapid Synthesis of Polyanhydrides by Microwave Polymerization. *Macromol Rapid Commun*. **25**: 330-333. 2004.

19. Vogt, James C., D.J. Krahwinkel, et al. Gradual Occlusion of Extrahepatic Portosystemic Shunts in Dogs and Cats Using the Ameroid Constrictor. *Veterinary Surgery*. **25**: 495-502. 1996.

20. Watkins, Anderew W., and Kristi S. Anseth. Copolymerization of photocrosslinkable anhydride monomers for use as a biodegradable bone cement. *J Biomater Sci Polymer Edn*. **14**: 3, 267-278. 2003.

21. Youmans, K. Ruth and Geraldine B. Hunt. Experimental Evaluation of Four Methods of Progressive Venous Attenuation in Dogs. *Veterinary Surgery*. **28**: 38-47. 1999.

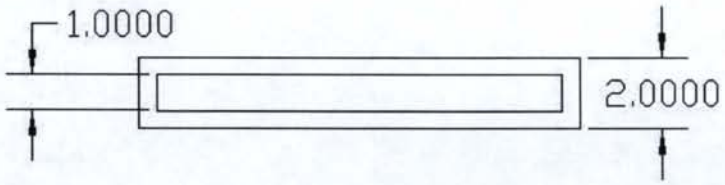

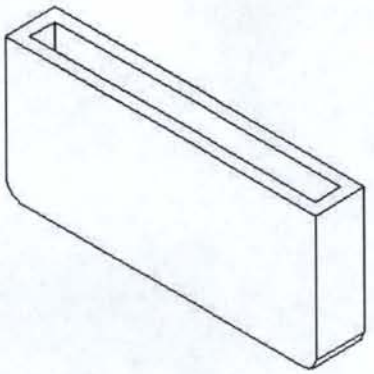

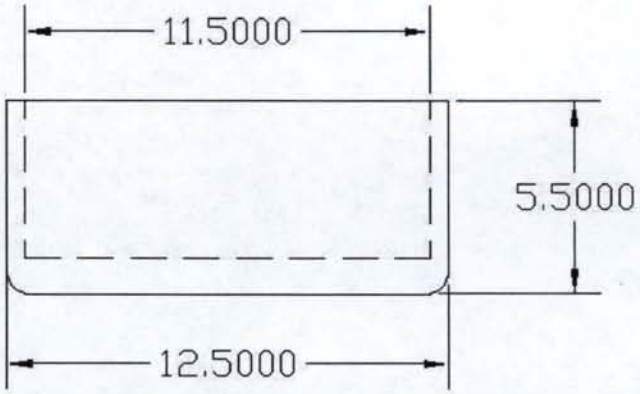

Appendix I - A: Occluder Pressure Plate

Millimeters
±0.01 unless otherwise noted

Geoff, Beth, Devin, Mitch

May 2, 2005

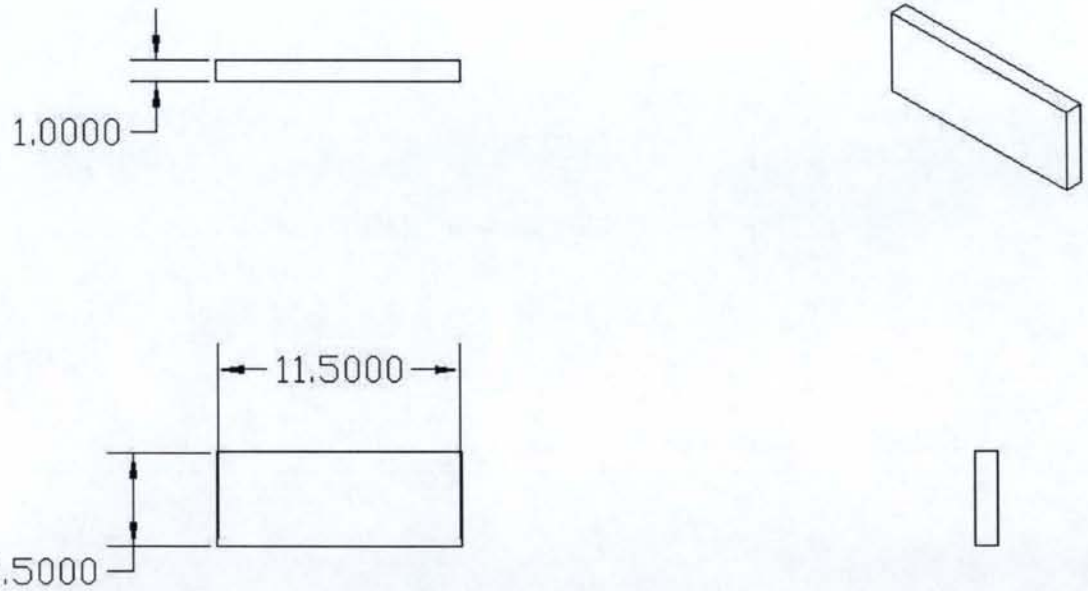

Appendix I-B: Hydrogel

Geoff, Beth, Devin, Mitch

May 2, 2005

Millimeters
±0.01 unless otherwise noted

XX

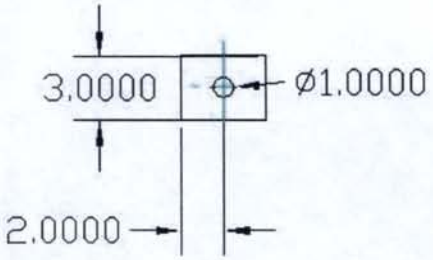

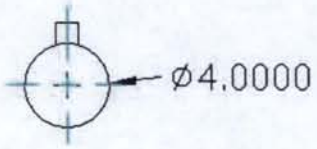

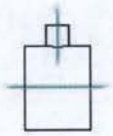

Appendix I-C: Biodegradable Polymer

Geoff, Beth, Devin, Mitch

May 2, 2005

Millimeters
±0.01 unless otherwise noted

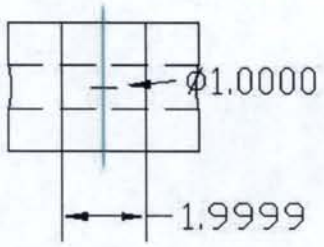

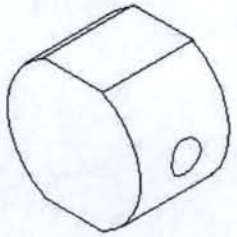

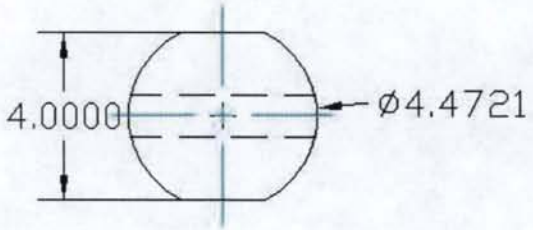

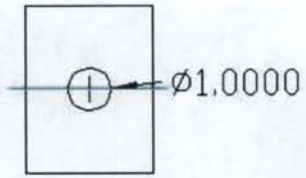

Appendix I-D

Appendix I- D: Occluder Circular Lock

Millimeters
±0.01 unless otherwise noted

Geoff, Beth, Devin, Mitch

May 2, 2005

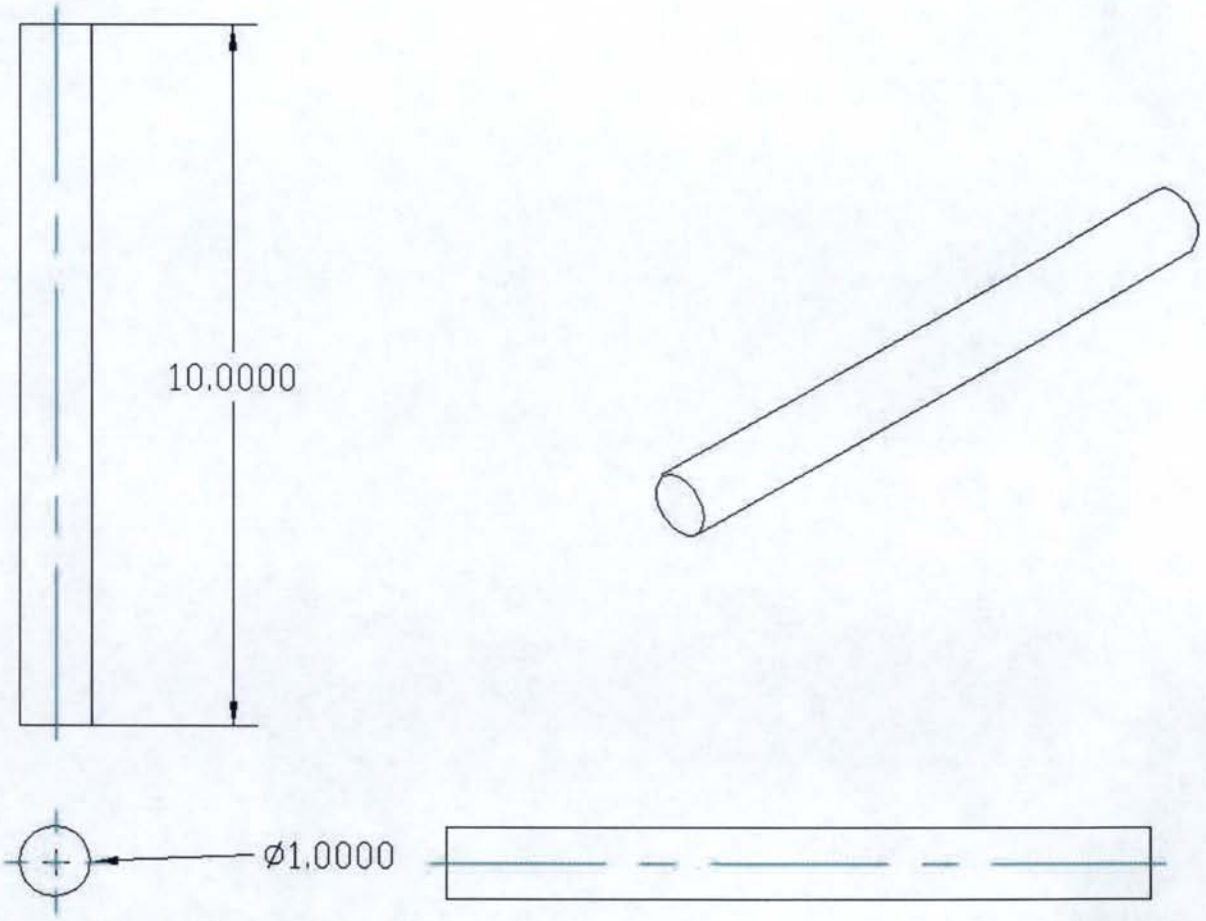

Appendix I- E: Rod Lock

Millimeters
±0.01 unless otherwise noted

Geoff, Beth, Devin, Mitch

May 2, 2005

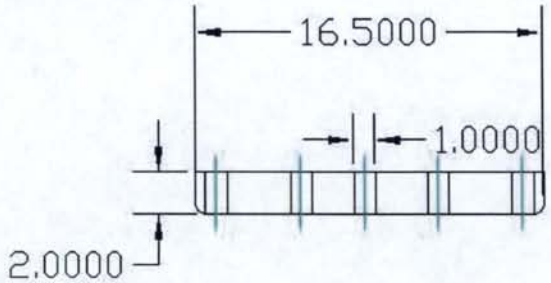

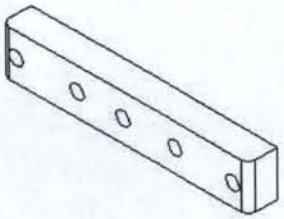

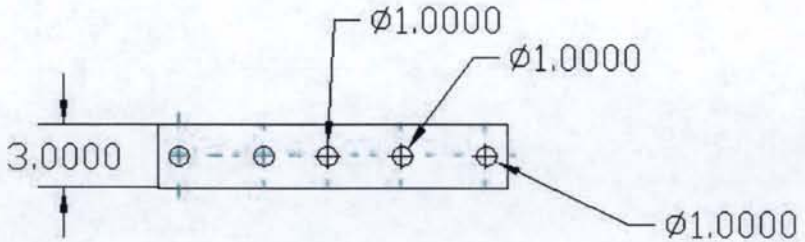

Appendix I-F

Appendix I- F: Occluder Top

Geoff, Beth, Devin, Mitch

May 2, 2005

Millimeters
±0.01 unless otherwise noted

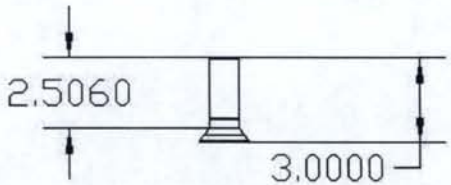

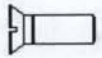

Appendix I-G: Countersunk Screw

Geoff, Beth, Devin, Mitch

May 2, 2005

Millimeters
±0.01 unless otherwise noted

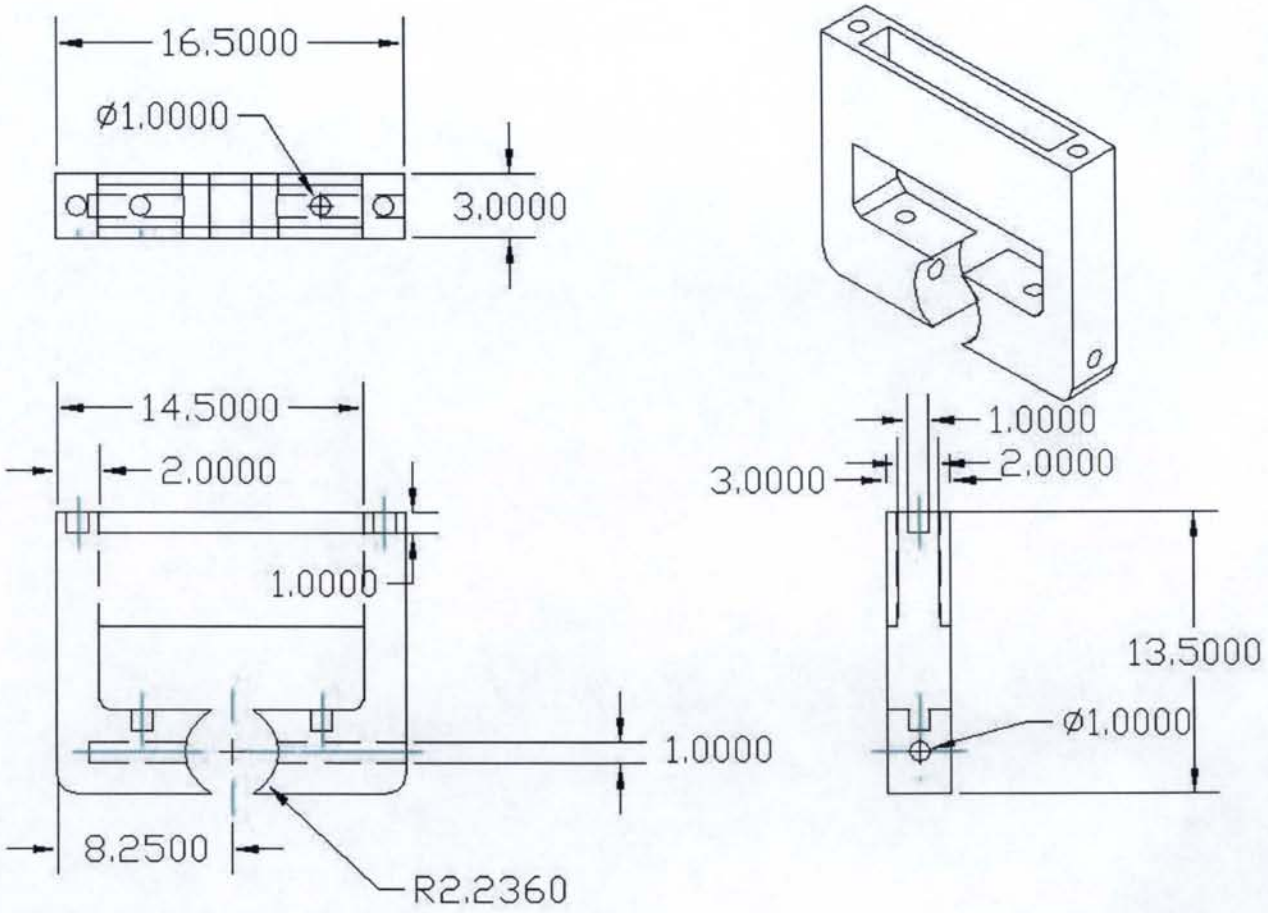

Appendix I- H: Occluder Casing

Millimeters
±0.01 unless otherwise noted

Geoff, Beth, Devin, Mitch

May 2, 2005

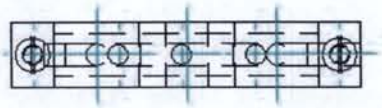

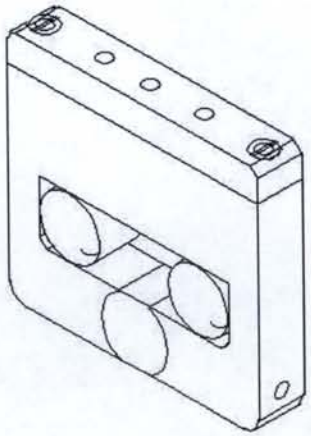

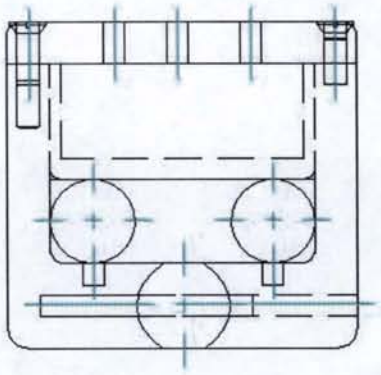

Appendix I-I: Occluder

Geoff, Beth, Devin, Mitch

May 2, 2005

Millimeters
±0.01 unless otherwise noted

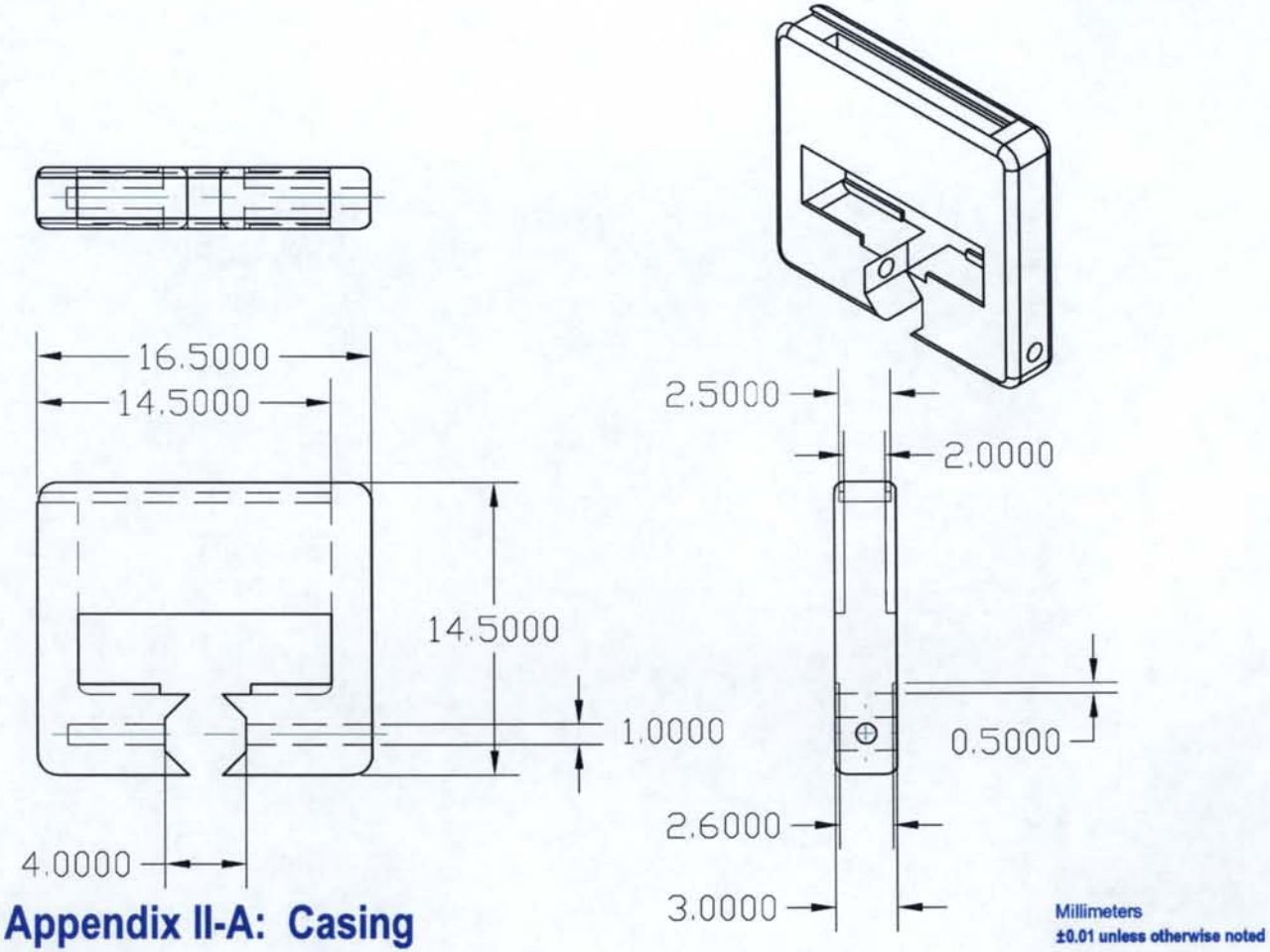

Appendix II-A: Casing

Geoff, Beth, Devin, Mitch

May 2, 2005

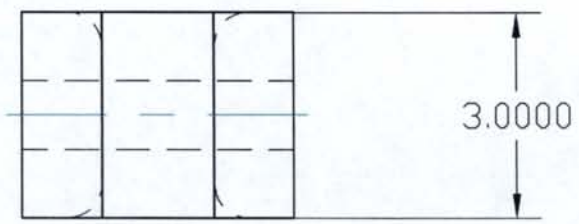

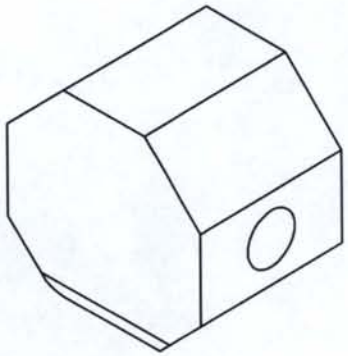

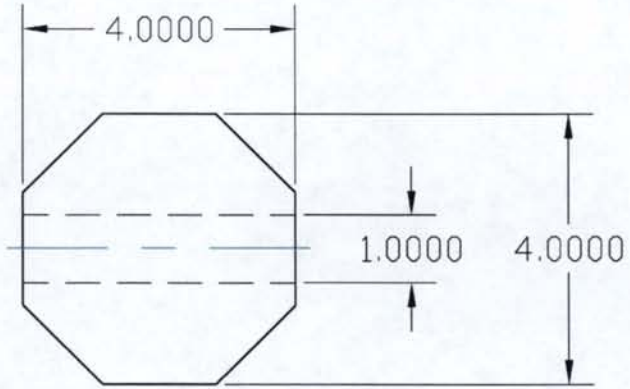

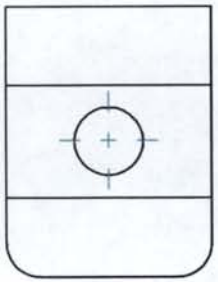

Appendix II- B: Occluder Hexagon Lock

Millimeters
±0.01 unless otherwise noted

Geoff, Beth, Devin, Mitch

May 2, 2005

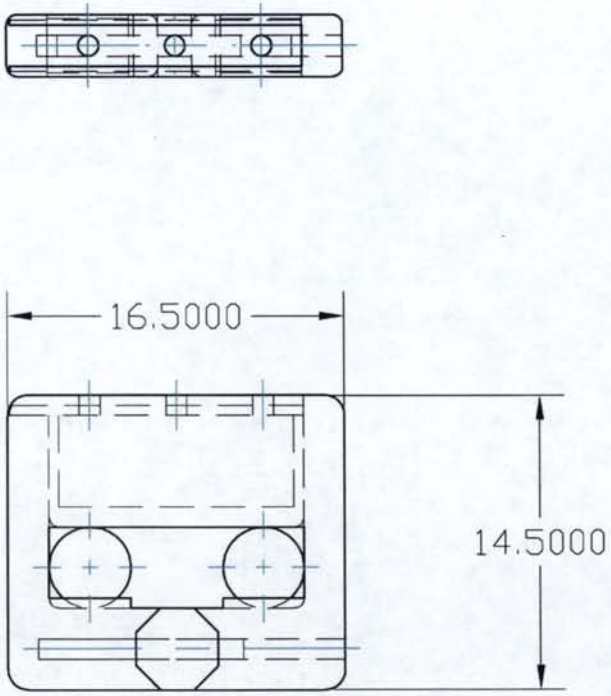

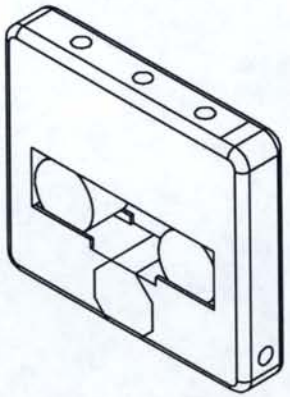

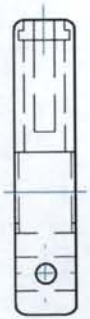

Appendix II-C: Origional Occluder

Geoff, Beth, Devin, Mitch

May 2, 2005

Millimeters
±0.01 unless otherwise noted